INFORMATION TO USERS

This manuscript has been reproduced from the microfilm master. UMI films the text directly from the original or copy submitted. Thus, some thesis and dissertation copies are in typewriter face, while others may be from any type of computer printer.

The quality of this reproduction is dependent upon the quality of the copy submitted. Broken or indistinct print, colored or poor quality illustrations and photographs, print bleedthrough, substandard margins, and improper alignment can adversely affect reproduction.

In the unlikely event that the author did not send UMI a complete manuscript and there are missing pages, these will be noted. Also, if unauthorized copyright material had to be removed, a note will indicate the deletion.

Oversize materials (e.g., maps, drawings, charts) are reproduced by sectioning the original, beginning at the upper left-hand corner and continuing from left to right in equal sections with small overlaps. Each original is also photographed in one exposure and is included in reduced form at the back of the book.

Photographs included in the original manuscript have been reproduced xerographically in this copy. Higher quality 6" x 9" black and white photographic prints are available for any photographs or illustrations appearing in this copy for an additional charge. Contact UMI directly to order.

U·M·I

University Microfilms International
A Bell & Howell Information Company
300 North Zeeb Road, Ann Arbor, MI 48106-1346 USA
313/761-4700 800/521-0600

Order Number 9405597

Thermodynamic and hydrodynamic behavior of the tissue factor:factor VII(a) complex

Waxman, Evan, Ph.D.

City University of New York, 1993

U·M·I
300 N. Zeeb Rd.
Ann Arbor, MI 48106

THERMODYNAMIC AND HYDRODYNAMIC BEHAVIOR OF THE TISSUE FACTOR:FACTOR VII(a) COMPLEX

by

EVAN WAXMAN

A dissertation submitted to the Graduate Faculty in Biomedical Sciences in partial fulfillment of the requirements for the degree of Doctor of Philosophy, The City University of New York

1993

This manuscript has been read and accepted for the Graduate Faculty in Biomedical Sciences in satisfaction of the dissertation requirement for the degree of Doctor of Philosophy.

6/16/93
Date

Cochairman of Examining Committee

6/16/93
Date

Cochairman of Examining Committee

6/22/93
Date

Executive Officer

Massimo Sassaroli

William R. Laws

L. Davenport

Supervisory Committee

The City University of New York

Abstract

THERMODYNAMIC AND HYDRODYNAMIC BEHAVIOR OF
THE TISSUE FACTOR:FACTOR VII(a) COMPLEX

by

Evan Waxman

Advisors: Dr. Yale Nemerson, Dr. J.B. Alexander Ross

The initial event in the extrinsic pathway of blood clotting is the formation of a complex between factor VII(a) and its cofactor, tissue factor (TF). This work concerns the thermodynamics and hydrodynamics of TF:VII(a) complex.

Concerning the thermodynamics of the complex we find that the isolated, extracellular domain of tissue factor (TF_{1-218}; sTF) exhibits 4% of the activity of wild-type TF (TF_{1-263}). Further, this activity is manifest only when vesicles consisting of phosphatidylserine and phosphatidylcholine (30/70, w/w) are present. To determine whether this decrease results from weakened affinity, we studied their interaction using ultracentrifugation, fluorescence anisotropy, and activities. Ultracentrifugation of the

sTF:VIIa complex established a 1:1 stoichiometry and an upper limit of 1 nM for the dissociation constant (K_d). This value agrees with titrations of dansyl-D-Phe-L-Phe-Arg-chloromethyl ketone active-site-labelled VIIa (DF-VIIa) with sTF using dansyl fluorescence anisotropy as the observable. Pressure dissociation was used to obtain quantitative values for binding. These experiments indicate that the K_d for the interaction of sTF with DF-VIIa is 0.59 nM (25° C). This value may be compared to a K_d of 7.3 pM obtained for the interaction of DF-VIIa with TF_{1-263} in phosphatidylcholine vesicles. The molar volume change of association was found to be 63 and 117 mL mol^{-1} for the interaction of DF-VIIa with sTF and TF_{1-263}, respectively. These binding data show that sTF:VIIa is quantitatively and qualitatively different from TF_{1-263}:VIIa.

Ultracentrifugation and fluorescence anisotropy decay techniques were used to evaluate the hydrodynamics of VIIa and sTF:VIIa. Sedimentation velocity experiments showed that both VIIa and sTF:VIIa are highly asymmetric. In each case, the friction ratio, f/f_{sphere}, is consistent with a family of ellipsoids ranging from prolate to oblate. Anisotropy decay experiments were then used to limit the family of ellipsoids which can describe the hydrodynamic behavior of VIIa and sTF:VIIa. For both VIIa and sTF:VIIa, the oblate ellipsoid of revolution was eliminated. The fluorescence anisotropy decay data show that upon binding sTF, VIIa loses a segmental motion involving a domain containing its active site.

Dedication

To my parents, Carl and Marilyn Waxman, who instilled in me the desire to learn and to my wife, Laura Smith, who provided the love, encouragement and support which made this work possible.

Acknowledgments

My most sincere appreciations to those who helped make this document and the work it represents possible. It is difficult to describe the debt I owe to my advisors Dr. Yale Nemerson and Dr. J.B. Alexander Ross. Their generosity of support in time spent, materials provided, patience and friendship were immeasurable.

Thanks to Dr. William Laws who acted as an unofficial thesis advisor and a good friend throughout my graduate school years. Thanks to Dr. Arabinda Guha for absolutely instrumental protein preparations and for the equally instrumental advice. Dr. Thomas M. Laue, in whose laboratory many of the key advances in this work were made, also deserves heartfelt thanks.

Thanks to Dr. Carol Hasselbacher, Paul Contino, and Elena Rusinova for helpful discussions, important technical assistance, and the occasional glass of cognac.

The tissue factor used in this work was provided by Dr. William Konigsberg's lab at Yale, New Haven.

I would also like to thank Dr. P. Katsoyanis and the Department of Biochemistry at Mt Sinai. Finally, thanks go to Dr. Terry Krulwich for her patience, support, and, of course, my introduction to the Nemerson and Ross labs.

Table of Contents

Title Page i

Approval Page ii

Abstract iii

Dedication v

Acknowledgements vi

Table of Contents vii

List of Figures viii

Chapter 1 - General Introduction 1
References 21

Chapter 2 - Pressure as a Thermodynamic Perturbant 23
References 45

Chapter 3 - Tissue Factor and Its Extracellular Soluble Domain: The Relationship between Intermolecular Association with Factor VIIa and Enzymatic Activity of the Complex 46
References 68

Chapter 4 - Human Factor VIIa and Its Complex with Soluble Tissue Factor: Evaluation of Asymmetry and Conformational Dynamics by Ultracentrifugation and Fluorescence Anisotopy Decay Methods 71
References 102

Chapter 5 - Summary and Further Discussion 105

References 112

List of Figures and Tables

Figure 1-1. A simplified diagram of the tissue factor initiated coagulation pathway . 3

Figure 1-2. Primary sequence of human tissue factor. 8

Figure 2-1. The Born replusion function 28

Figure 2-2. Schematic diagram of the high-pressure spectroscopy apparatus 33

Figure 2-3. Pressure dissociation curve for a heterodimeric association reaction . . 36

Figure 2-4. Effect of ΔV on a graph of *versus* P. 38

Figure 2-5. Effect of $K_{d,atm}$ on a graph of α *versus* P 39

Figure 2-6. Effect of concentration on a graph of α *versus* P 40

Figure 2-7. Comparison of pressure dissociation of a heterodimer and pressure denaturation curves 44

Figure 3-1. Fluorescence anisotropy titration of DF-VIIa with sTF and TF_{1-263}. . . . 58

Figure 3-2. Pressure dissociation curve of sTF:DF-VIIa and TF_{1-263}:DF-VIIa complexes 60

Figure 3-3. Titration of VIIa with sTF. 62

Figure 4-1. Flow diagram for evaluation of hydrodynamic parameters 75

Figure 4-2. Representation of a general ellipsoid 76

Table 4-1. Calculation of hydrodynamic parameters 91

Figure 4-3. Flatness (b/c) versus elongation for the family of ellipsoids consistent with the friction ratios determined for VIIa and sTF:VIIa 93

Figure 4-4. Correlation times versus η/RT for DF-VIIa and sTF:DF-VIIa 96

Table 4-2. Time-Resolved fluorescence anisotropy parameters 97

CHAPTER 1

GENERAL INTRODUCTION

Background.

The initial event in the extrinsic pathway of blood clotting (figure 1-1) is the formation of a complex between the serum apoenzyme factor VII(a)[1] and its membrane-bound cofactor, tissue factor (TF). The holoenzyme, TF-VII(a), proteolytically activates the clotting cascade zymogens factor X and factor IX, initiating the series of proteolytic cleavages that results in the cleavage of fibrinogen and formation of a fibrin clot. The formation of the TF-VII(a) complex is the trigger event in the clotting cascade.

A number of detailed reviews of the biochemistry of factor VII(a), TF, and the role of the TF-VII(a) complex in the extrinsic pathway of blood coagulation are available (Zur and Nemerson, 1981; Bach, 1988; Nemerson, 1988). In addition, several review articles cover the coagulation system in general (Davie, 1986; Jackson and Nemerson, 1980). Highlights relevant to this study are presented here.

Factor VII.

Factor VII is a single-chain glycoprotein with a molecular weight of about 50,000. It is one of several vitamin K-dependent serine proteases involved in the thrombogenic pathway. Others include factor IX and factor X, substrates of the TF-VII(a) complex; prothrombin, the precursor of thrombin; and protein C, an anticoagulant protease that inactivates factor V and factor VIII. This class of proteins share a number of features.

1) The site of synthesis for these proteins is the liver.

---

[1]Throughout this document "VII(a)" will be used as shorthand for "VII or VIIa". "VII" and "VIIa" will be used when differences between the zymogen and activated forms of the enzyme are being discussed.

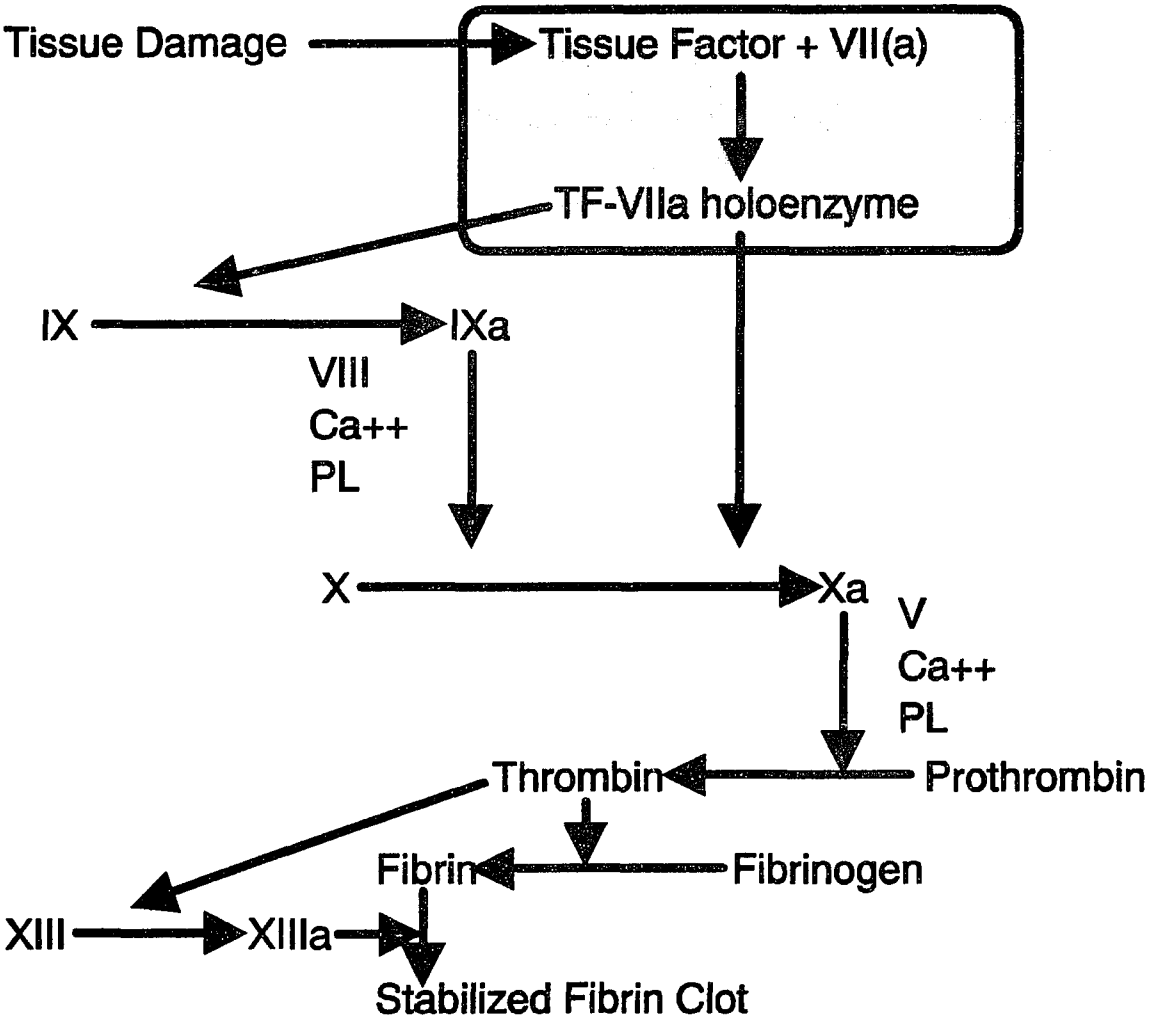

Figure 1-1. A simplified diagram of the tissue factor initiated coagulation pathway.

2) They require gamma-carboxylation of several specific amino terminus glutamic acid residues for activity. The enzyme catalyzing this reaction requires vitamin K.

3) They share a large degree of sequence homology in their amino terminal segments. These segments are responsible for Ca^{2+}-dependent binding to phospholipid.

4) The serine protease active site of these proteins is located at the carboxyl terminal. In this region, these proteins share a large degree of homology with the more general class of serine proteases which include trypsin and chymotrypsin.

5) They circulate as zymogens and are activated by proteolytic cleavage at specific sites. In some cases activation is accompanied by release of an activation peptide.

6) The vitamin K-dependent serine proteases have extended specificity compared to trypsin and chymotrypsin. Each will catalyze the proteolytic cleavage of only a small number of specific sequences on specific proteins. Cross-reactivity between these proteins is limited.

Factor VII is unique among the vitamin K dependent-serine proteases in several ways.

1) It has unusually high activity (~1%) in its zymogen form.

2) Factor VII has an absolute requirement for its cofactor TF for activity. The binding of VII(a) to TF is accompanied by an increase of nearly three orders of magnitude in the activity of VII(a). Unlike the cofactors, factor V and factor VIII,

TF is not present in plasma. It is accessible only at sites of tissue damage.

3) Factor VII is present in plasma in only trace concentrations. The circulating concentration of VII is approximately 13 nM in bovine plasma and 10 nM in human plasma.

These features are all appropriate for the role of factor VII in triggering coagulation and suggest the following, widely accepted, scheme for the initiation of clotting. Tissue damage causes the exposure of TF to the blood. Factor VII subsequently binds to TF. This minimally active complex activates factor X or factor IX. Factor Xa or factor IXa are then capable of converting factor VII, perhaps while still attached to TF, to its more active form, VIIa. In addition, there is evidence that the presence of substrate increases the affinity of VII for TF. The fully activated, high-affinity form of TF-VIIa then proceeds with maximal activation of IX or X until shut down by a variety of feedback mechanisms.

VII is activated by proteolytic cleavage of a specific Arg-Ile site. The resulting two chain form of the enzyme, VIIa, is linked by a disulfide bond. No activation peptide is released by the conversion of VII to VIIa. Factor IXa, factor Xa, thrombin and factor XIIa have all been shown to be capable of activating VII. The relative roles for these activators *in vivo* are not known.

Factor VII has been approximately 200,000-fold purified from bovine (Bach *et al.*, 1984) and human plasma (Broze and Majerus, 1980). Purification is complicated by: the trace plasma concentrations of VII; the presence, in the plasma, of both the zymogen and

activated forms of the enzyme; the relatively larger concentrations of the other vitamin K-dependent serine proteases from which it must be separated; and by the sensitivity of VII to proteolytic degradation by a variety of plasma enzymes. Initial purification required the use of benzamidine as an affinity chromatography ligand and the presence of proteolytic inhibitors throughout the isolation procedure for success. Purification of bovine VII from plasma has recently been improved by the use of an immunoabsorbent column (Bach *et al.*, 1984).

Recently, the sequence of human VII(a) has been deduced from cDNA clones (Hagen *et al.*, 1986) and the protein has been successfully expressed in a mammalian cell line (Berkner *et al.*, 1986). Expression in a mammalian cell line is necessary for producing active VIIa as bacteria lack the vitamin K-dependent enzyme necessary for gamma carboxylation of amino-terminal glutamic acid residues.

Tissue Factor

Tissue factor is an integral membrane protein with a molecular weight of approximately 45,000. The protein is rich in carbohydrates, but these may be removed without any loss of activity *in vitro*. There is no known primary sequence homology between TF and any other sequenced protein. In particular, TF is not homologous to factor V or factor VIII, the cofactors involved in reactions catalyzed by factor X and factor IX, respectively.

TF is produced constitutively by several cell types including fibroblasts and smooth muscle cells. TF is not, however, normally produced by cells that are in contact

with plasma. There is evidence that TF expression can be induced in endothelial cells and monocytes in tissue culture by a number of different stimuli. The role for this inducible production of TF *in vivo* is unclear.

The primary sequence of TF suggests its division into three domains (figure 1-2). The first 219 residues form the extracellular domain. These are followed by a hydrophobic membrane-spanning domain (residues 220-242). A cytoplasmic domain is formed by the remaining twenty residues (243-263). The extracellular domain contains four half-cystines linked into two disulfide bonds. These disulfides are necessary for activity. The cytoplasmic domain contains an additional half-cystine. Three N-linked carbohydrate attachment sites exist in the extracellular domain.

Until recently, TF was usually isolated from brain tissue for biochemical studies. The protein was extracted from brain acetone powder using Triton X-100. The protein was then purified on either an immunoaffinity column or an agarose-linked factor VII column (Bach *et al.*, 1981; Broze *et al.*, 1985; Guha, *et al.*, 1986).

In 1987, a number of groups isolated the cDNA sequence for human TF (Spicer *et al.*, 1987; Morrisey *et al.*, 1987; Scarpati *et al.*, 1987). This was followed by the introduction of the TF structural gene into bacterial cell lines capable of overexpressing the protein (Fisher and Gorman, 1981). This development has made milligram quantities of TF available.

The recovery of maximal activity from purified TF preparations depends on reconstitution into phospholipid vesicles. This is generally accomplished by the detergent dialysis technique (Bach *et al.*, 1986). TF is combined with phospholipid in the presence

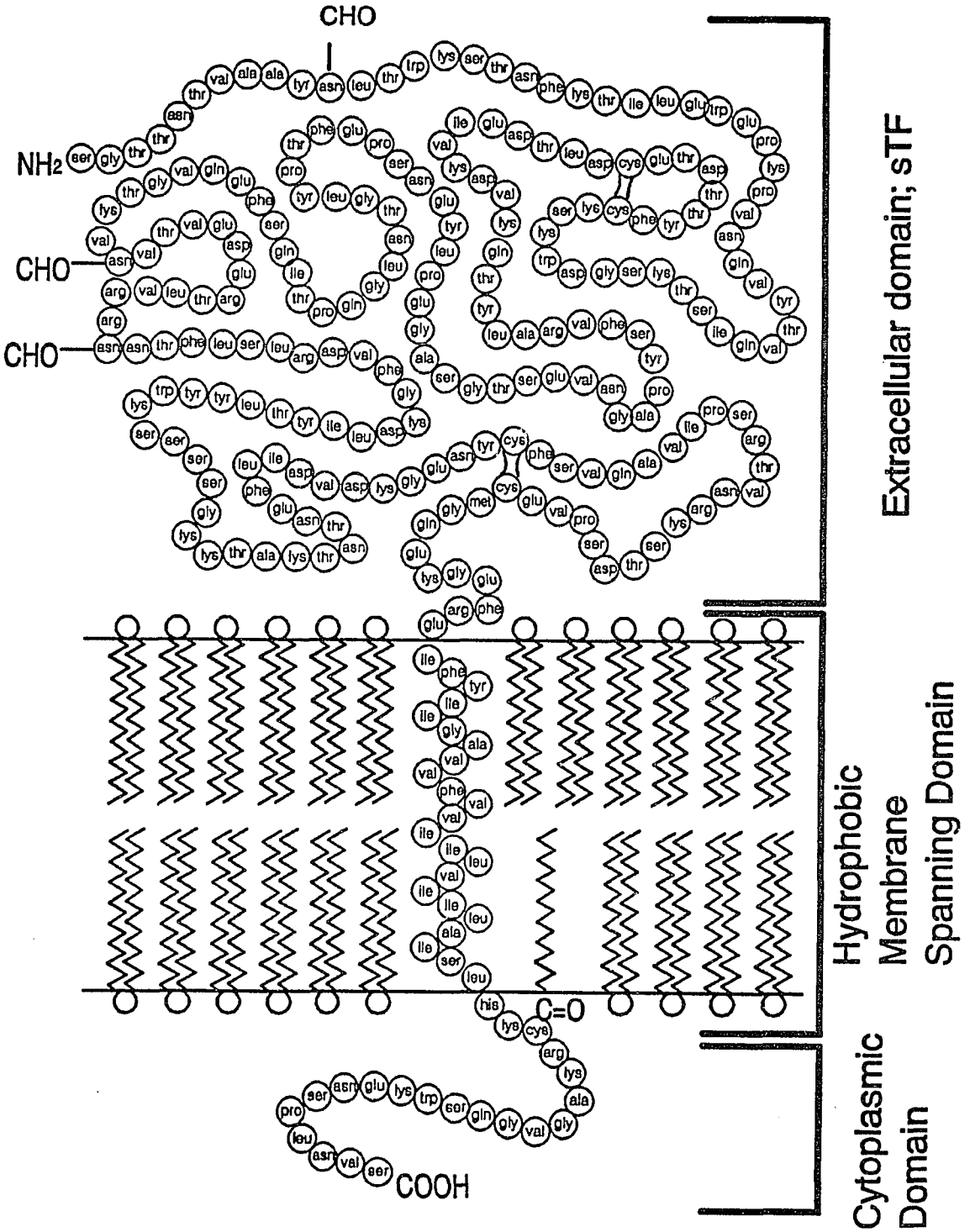

Figure 1-2. Primary sequence of human tissue factor, demonstrating division in cytoplasmic, membrane spanning and extracellular domains.

of a large excess of the detergent beta-octylglucoside. The preparation is dialyzed to remove the detergent. The resulting vesicles are then sized on a gel filtration column. Vesicles produced by this method have diameters between 100 and 200 nanometers and are unilamellar.

Previous studies of TF:VIIa binding.

The unique position of TF:VIIa complex formation in the clotting cascade, the nearly three orders of magnitude increase increase in the activity of VIIa when it is bound to TF, and the small concentrations of TF:VIIa required to quickly form a macroscopic clot have directed considerable attention to the study of TF:VIIa complex formation.

Blood cells are, in general, devoid of tissue factor activity; however, some studies (Lerner, *et al.*, 1971) suggested that endotoxin could cause an enhancement of coagualant activity of monocytes in the prescence of lymphocytes. In a study by Broze (1982), the binding of VII and VIIa to TF present on monocytes was examined. The purpose of this study was to test whether this response could be correlated with the presence of VII(a) binding sites on the monocyte cell surface. Monocytes, activated by overnight incubation with endotoxin, were combined with ^{125}I VII(a) and allowed to incubate for 60 minutes at 0, 20, or 37° C. The 60 minute incubation period was chosen after preliminary experiments showed that the binding of ^{125}I VII(a) to monocytes was time dependent but reached a maximum value after this amount of time. Free VII(a) was separated from bound by a two step centrifugation procedure. First, an aliquot of the labelled VII(a)-

monocyte mixture was centrifuged at ambient temperature for two minutes in a microfuge. Subsequently, N-butyl-pthalate was layered over the sample and the sample was centrifuged for an additional two minutes. Free VII(a) was determined by measuring the radioactivity present in an aliquot taken from the supernatant above the oil layer. The remainder of the supernatant and the oil were removed. Bound VII(a) was determined by measuring the radioactivity present in the cell pellet.

The number of sites for VII(a) binding were evaluated from a graph of bound ^{125}I VII(a) versus ^{125}I VII(a) added. Dissociation constants were determined from a double reciprocal plot (1/bound versus 1/free). At 0° C, the number of binding sites per monocyte was determined to be 3600. The dissociation constant for both labelled VII and labelled VIIa at this temperature was approximately 82 pM. The graphs of the 37° C data indicated that processes other than simple binding were occuring. The number of binding sites per monocyte appeared to be at least three times that observed at 0° C but saturation was not reached. No attempt was made to evaluate the 37° C data for a dissociation constant. Competition experiments were performed with unlabelled VII and VIIa. The competitive inhibition constants (K_i's) obtained for the unlabelled proteins were essentially identical to the dissociation constants (K_d's) obtained for the iodinated proteins. An assay of the reaction mixtures for X activation showed that binding was well correlated with activity.

Some of the difficulties inherent in the measurement of tight binding interactions are exemplified by this study. First, the concentration of VII(a) present at saturation was approximately 400 pM. Approximately 20% binding was detected when the total

concentration of labelled VII(a) was only 20 pM. These concentrations test the limits of detectability of even ^{125}I. Perhaps more importantly, VII(a) is known to stick to a variety of glass and plastic surfaces. At high concentrations of protein the percentage of material lost to pipette tips, test tubes, etc., is probably small; however, at concentrations in the pM range it is difficult to estimate how much VIIa actually remains in solution. The accuracy of any evaluation of the dissociation constant can at best be as good as the accuracy to which the concentration of VII(a) is known.

Two other issues relevant to the examination of other studies of TF:VIIa binding are well illustrated by this study. First, the procedure used in this study required separation of free VII(a) from bound VII(a). This separation took place over a period of minutes and at a temperature different from that at which equilibrium was established. The separation technique is therefore guaranteed to perturb the equilibrium. The dilution caused by the separation process will cause the amount of VII(a) bound at equilibrium to be underestimated and the amount free to be overestimated. In addition, the interval during which the solution is at increased temperature will similarly perturb the equilibrium, depending on the signs and magnitudes of ΔH and ΔS. The value of 82 pM obtained is therefore likely to underestimate the tightness of this interaction.

The second issue concerns the inability of the procedure used in this study to evaluate the TF:VIIa interaction as a function of temperature. While this inability did not adversely effect Broze's capacity to conclude that TF:VIIa activity was well correlated with binding of VIIa to the monocyte surface, it is clear that this is not the method of choice for a detailed study of the thermodynamics of the TF:VIIa interaction.

In a 1984 study by Rodgers et al., the binding of VII(a) to TF present on the surface of a variety of cultured nonvascular cell lines was examined. The purpose of this study was to further establish a correlation between VII(a) binding and apparent TF:VII(a) activity. The cell lines that showed significant amounts of VII(a) binding were bovine corneal endothelium (BCE) cells, human newborn foreskin fibroblasts, and fetal lung cells. In these experiments, cultured cells were first washed twice with chilled Dulbecco's modified essential medium (DMEM) containing 0.5% bovine serum albumin (BSA). After washing, DMEM plus BSA was added to bring the volume to 1 ml. ^{125}I VII(a) was then added to the cells to a final concentration ranging from 0.1 nM to 6 nM. The culture was allowed to incubate for 1-2 hr at 4° C. As in the study by Broze (1982), the incubation time was chosen because preliminary experiments indicated that binding was not complete at times less than 1 hr. 4°C was chosen for the incubation time as binding was nonsaturable at 37°C. Free VII(a) was separated from VII(a) bound to the cell surface by washing the culture three times with a chilled phosphate buffered saline solution containing 0.1% BSA. The cells were subsequently solubilized and the amount of bound VIIa was determined by measurement of radioactivity.

Analysis of the data indicated that the cell lines differed widely with respect to the amount of VIIa bound per cell at saturation and their binding affinities for VII(a). The BCE cells demonstrated both the lowest number of binding sites per cell (2400 sites cell^{-1}) and the tightest association (K_d = 130 pM). The fetal lung cells had the greatest number of molecules bound per cell at saturation (880,000 sites cell^{-1}) and the lowest affinity for VII(a) (K_d = 9 nM). The fibroblasts exhibited the intermediate values of 14,000 sites

$cell^{-1}$ and K_d = 400 pM. By comparing the binding data to the rate at which the cultured cells generated Xa the authors were able to conclude that activity is directly related to the amount of VII(a) bound irrespective of the difference in affinities observed.

The approach used in this study is similar to that used in the previous study by Broze (1982). Measurement of binding requires separation of bound and free VII(a), with concomitant destruction of equilibrium conditions. In addition, very dilute solutions are required in order to span the realm from no binding to saturation; and temperature studies are rendered impossible due to nonsaturability at high temperatures.

In a 1986 study, Bach *et al.* examined the binding of tritiated VII(a) to purified bovine TF reconstituted in vesicles. The composition of the vesicles ranged from pure phosphatidylcholine (PC) and to mixtures of phosphatidylserine (PS) and phosphatidylcholine containing 40% PS. Lipid to TF ratios varied from 75,000:1 to 110,000:1 in the different lipid preparations. Labelled VII(a) was incubated with TF for 30 minutes at 37° C. Bound VII(a) was separated from free by floatation through a discontinuous gradient of 20%, 10% and 5% sucrose. Samples were centrifuged at 150,000g for 10 min. Binding was evaluated by measurement of the radioactivity present in the uppermost and lowermost layers of the sample after centrifugation. Corrections were applied to the measured amounts to account for incomplete separation of vesicles, nonspecific binding, and mixing of bound and free pools.

One-to-one stoichiometry was observed for all experiments. The corrected data were fit to a simple one-site binding model. Data obtained from samples containing

vesicles composed of 100% PC fit this model well and dissociation constants of 13.2 nM and 4.5 nM were obtained for VII and VIIa, respectively.

Data obtained from samples containing TF reconstituted in PS:PC vesicles did not fit well to a simple one site binding model. Scatchard analysis of these data showed curvature suggestive of positive cooperativity. Good fits were observed when the data were fit using the Adair two-site cooperative model. The $K_{1/2}$ obtained from Hill plot analysis decreased from 12.2 to 0.66 nM for VII and from 4.27 to 1.69 nM for VIIa as the percentage of PS was varied from 5 to 40%.

Bach *et al.* also examined the binding of diisopropylphosphorous (DIP) active site labelled VII(a) to TF. The binding of DIP-VII and DIP-VIIa was tighter than that of the corresponding untreated protein for all lipid compositions studied. This suggests that modification of the active site of VII(a) may induce a conformational change that results in tighter binding to TF. This issue was pursued further in a companion paper by Nemerson and Gentry (Nemerson and Gentry, 1986). In this paper, the kinetics of the activation of X to Xa by the TF:VIIa complex was examined under conditions where significant amounts of free VIIa and free TF are present. The data demonstrate a dramatic decrease in the $K_{1/2}$ for VIIa and TF when substrate concentration is increased, indicating that the prescence of substrate inhibits the dissociation of the TF:VIIa complex. The dissociation constant calculated by fitting initial velocity data to the ordered addition model

$$A+E \underset{k_{+1}}{\overset{k_{-1}}{\longleftrightarrow}} AE + S \underset{k_{+2}}{\overset{k_{-2}}{\longleftrightarrow}} AES \xrightarrow{k_{cat}} P+AE$$

where A,E,S, and P are activator, enzyme, substrate and product respectively, was estimated to be between 40 and 90 pM, approximately 2 orders of magnitude below the value determined by Bach *et al.* using the centrifugation binding assay.

A 1987 study by Fair and MacDonald makes use of a procedure essentially identical to that used by Rodgers *et al.* (1984) to study the binding of ^{125}I VII(a) to the surface of the J82 bladder carcinoma cell line. These investigators determined a dissociation constant 222±85 pM and an average of 38,300±14,300 binding sites cell^{-1}. In contrast to the studies by Broze (1982) and Rodgers *et al.* (1984), these investigators observed saturation of binding sites at 37° C. In addition, the binding isotherm was found to be sigmoidal, suggesting positive cooperativity. It is possible, however, that the data were somewhat overinterpreted in light of the fact that over 50% of the total binding observed was shown to be nonspecific.

A 1987 study by Ploplis *et al.* uses the identical procedure to study VII(a) binding to a human fetal lung cell line. The results of this study are in agreement with the those of the study by Fair and MacDonald (1987) with regard to the saturability of the specific

VII(a) binding sites at 37°C . However no cooperativity was observed for binding to this cell line. As in the Fair and MacDonald study, nonspecific binding was seen to be responsible for more than 50% of total binding. The dissociation constant determined by this study was 123±37 pM.

Finally, a quite recent study by Ruf *et al.* (1991) examined the binding of ^{125}I VII(a) to TF purified from human brain and a soluble TF construct lacking the cytoplasmic and membrane spanning domains of native TF. In this study, TF and labelled VIIa were added to microtiter wells coated with an antibody to TF. Samples were incubated for 90 min at 37°C and then washed with ice-cold TBS. Binding was evaluated by measurement of radioactivity present in the wells after washing. The dissociation constants obtained for the binding of VII and VIIa with native human brain TF were 9.2±3.5 and 4.2±2.6 nM respectively. The dissociation constants obtained for the binding to the soluble TF construct were 116±41.4 nM for VII and 90.3±26.5 nM for VIIa.

It is difficult to evaluate the quality of these data for several reasons. First, as with the other procedures examined so far, the procedure used in this study requires separation of free VII(a) from bound. It is thus not an equilibrium measurement. Second, the antibody used in this procedure was shown in a previous paper (Morrissey *et al.*, 1988) by these authors to have an inhibitory effect on TF:VIIa binding. Third, in no experiment presented in the figures of this paper is saturation of TF reached. Other figures in this paper indicate that saturation of VIIa is not observed when proteolytic activation of X to Xa is followed as a function of TF concentration. Finally, despite the

title of this paper, "*Characterization of Factor VII Association with Tissue Factor in Solution*", it is not clear that the molecule of TF bound to a microtiter plate by an antibody is truly in solution. It is thus not surprising that the dissociation constant for TF:VIIa binding determined by this study is two orders of magnitude higher than that determined for any other study of the human TF:VII(a) complex.

Summary of the Problem and Approach.

As noted above, previous studies of the TF:VIIa interaction have reported dissociation constants ranging from 82 pM to 9 nM. Furthermore, some of these studies report evidence of lipid-dependent cooperativity while others report no evidence of cooperativity. The wide range of dissociation constants reported can be attributed to three major factors.

1) None of the techniques used in these studies are true equilibrium techniques. All require either separation of bound VIIa from free VIIa or calculation of dissociation constants from kinetic parameters. Separation of bound VIIa from free VIIa is guaranteed to perturb equilibrium unless performed instantaneously relative to TF:VIIa dissociation and association rates. Determination of dissociation constants using rate constants requires an excellent knowledge of the mechanism of interaction.

2) These studies used a variety of different TF preparations. In several of the studies TF present on human cell lines were studied. Significant variation in the dissociation constants were observed for different cell lines. Bach *et al.* (1986) examined purified bovine TF reconstituted in phospholipid. Ruf *et al.* (1991) examined TF purified

from human brain reconstituted in phospholipid or solubilized in Triton.

3) Accurate measurement of dissociation constants for a two-state system requires observation of at least 75% of the association curve (Deranleau, 1969). Ideally then, one should observe association from 10 to 90%. When concentrations are unknown as they were in the studies done on cell lines or microtiter plates, it is best to examine association greater than 90% so that the number of sites may be determined independently. As the dissociation constant for TF:VIIa binding appears to be 1 nM at most, observation of 10% association would require measurement of at most 12 pM complex. If in fact the dissociation constant is in the lower part of the reported range (~100 pM) observation of 10% binding would require measurement of 1.2 pM complex. Two problems exist in this case. First, accurate detection of these quantities of complex is extremely difficult to accomplish by any method and so a complete range of association fractions is difficult to achieve. Second, proteins in general, and the clotting factors in particular, are difficult to work with at these concentrations as they tend to be lost due to interactions with container surfaces, pipette tips, etc. The total concentration of TF and VIIa in any sample is therefore difficult to determine at low concentrations.

None of these "criticisms" are meant to imply that these studies were bad science. It was not the intent of any of these studies to provide a framework for a complete thermodynamic description of the TF:VIIa interaction. Furthermore, the concentration range problem is not solvable using any conventional approach. Nevertheless, it is clear that if we wish to determine the thermodynamic parameters of the TF:VIIa interaction

well enough to make conclusions about the types of forces involved, we will require a technique which will enable us to directly observe the degree of TF:VIIa association under equilibrium conditions. Dissection of enthalpic and entropic contributions to the free energy binding requires a technique which can be used over a wide range of temperatures and concentrations. The effect of factors such as calcium or lipid composition can only be determined by comparison to well-defined TF and VIIa standards. Furthermore, separation of effects due to protein-lipid interactions from those due to direct protein-protein interactions requires well-defined lipid preparations and a well-characterized method for reconstitution of TF. Under ideal conditions, the protein-protein interactions should be evaluated in the absence of lipid.

The Nemerson lab has many years of experience preparing, reconstituting and characterizing TF. The procedure used in this lab to reconstitute TF has become the standard throughout the field and the resulting TF-containing vesicles have been characterized with respect to size, TF orientation, and activity. In addition, this lab has prepared a recombinant TF construct which lacks the cytoplasmic and membrane spanning domains. This TF mutant (TF_{1-218}, soluble tissue factor, sTF) is soluble at concentrations up to at least 50mg/ml and has approximately 4% of the activity of wild-type TF.

In the study presented in chapter 3, wild-type TF:VIIa and sTF:VIIa association are measured using fluorescence anisotropy as an observable and high pressure as a thermodynamic perturbant. Fluorescence anisotropy provides a sensitive means for observing the state of association of labelled VIIa down to concentrations of approximately 50 nM. High pressure can be used to shift the dissociation constant into

the range where the TF:VIIa complex will be largely dissociated at concentrations measurable using fluorescence anisotropy. Chapter 2 describes high pressure dissociation methods in greater detail.

References for Chapter 1

Bach, R., Nemerson, Y., & Konigsberg, W. (1981) *J.Biol. Chem.* 256, 8324-8331.

Bach, R., Oberdick, J. and Nemerson, Y. (1984) *Blood*, 63, 393-398.

Bach, R., Gentry, R., & Nemerson, Y. (1986) *Biochemistry 25*, 4007-4020.

Bach, R. (1988) *CRC Crit. Rev. Biochem.* 23, 339-368.

Berkner, K., Busby, S., Davie, E., Hart, C., Insley, M., Kisiel, W., Kumar, A., Murray, M., O'Hara, P., Woodbury, R. (1986) *Cold Spring Harbor Symposia on Quantitative Biology* 51, 531-541.

Broze, G.J., and Majerus, M.J. (1980) *J. Biol. Chem.* 255, 1242-1247.

Broze, G.J., Jr. (1982) *J. Clin. Invest.*, 70, 526-535

Broze, G.J., Jr., Leykam, J.E., Schwartz, B.D., & Miletich, J.P. (1985) *J. Biol. Chem.* 260, 10917-10920.

Davie, E.W. (1986) *J. Protein Chem.* 5, 247-253

Deranleau, D. (1969) *J. Am. Chem. Soc.* 91 4044-4049.

Fair, D. S., & MacDonald, M. J. (1987) *J. Biol. Chem. 262*, 11692-11698.

Fisher, K.L., and Gorman, C.M. (1989) *Thromb. Res.* 48, 89-99.

Guha, A., Bach, R., Konigsberg, W., & Nemerson, Y., (1986) *Proc. Natl. Acad. Sci. U.S.A.* 83, 299-302.

Hagen, F.S., Gray, C.L., O'Hara, P., Grant, F.J., Saari, G.C., Woodbury, R.G., Hart, C.E., Insley, M., Kisiel, W. (1986) *Proc. Natl. Acad, Sci. U.S.A.* 83, 2412-2416.

Jackson, C. and Nemerson, Y. (1980) *Ann Rev. Biochem.* 49, 765-811.

Lerner, R.G., Goldstein, R., and Cummings, G. (1971) *Proc. Soc. Exp. Biol. Med.* 138, 145-148.

Morrisey, J.H., Fakhrai, H. and Edgington T.S. (1987) *Cell,* 50, 129-135.

Morrissey, J. H., Fair, D. S., & Edgington, T. S. (1988) *Thrombosis Research 52,* 247-261.

Nemerson, Y. (1988) *J. Am. Soc. Hematology* 71, 1-8.

Nemerson, Y. & Gentry, R. (1986) *Biochemistry* 25, 4020-4033.

Ploplis, V. A., Edgington, T. S., & Fair, D. S. (1987) *262*, 9503-9508.

Rodgers., G. M., Broze, G. J., & Shuman, M. A. (1984) *Blood 63*, 434-438.

Ruf, W., Kalnik, M. W., Lund-Hansen, T., & Edgington, T. S. (1991) *J. Biol. Chem. 266*, 15719-15725.

Scarpati, E.M., Wen D., Broze, G.J., Mileteich, J.P., Flandermeyer, R.R., Siegel, N.R., and Sadler, J.E. (1987) *Biochemistry*, 26, 5234-5238.

Spicer, E. K., Horton, R., Bloem, L., Bach, R., Williams, K. R., Guha, A., Kraus, J., Lin, T. C., Nemerson, Y., & Konigsberg, W. H. (1987) *Proc. Natl. Acad. Sci. U.S.A. 84*, 5148-5152.

Zur, M. and Nemerson, Y. (1981) *Haemostasis and Thrombosis*, A. L. Bloom and D. P. Thomas (Eds.), pp 124-142, Churchill Livingston, Edinburgh.

CHAPTER 2

HIGH PRESSURE AS A THERMODYNAMIC PERTURBANT

High pressure as a thermodynamic pertubant.

Consider the general chemical reaction:

$$n_{R_1}R_1 + n_{R_2}R_2 + \cdots \rightleftharpoons n_{P_1}P_1 + n_{P_2}P_2 + \cdots \quad (1)$$

in which n_{R1} moles of reagent R_1, n_{R2} moles of reagent R_2, and so on, are converted to n_{P1} moles of product P_1, n_{P2} moles of reagent P_2, and so on. The free energy change for this reaction at constant temperature and pressure, ΔG is given by

$$\Delta G = \sum_{i=1}^{N_P} n_{P_i}\mu_{P_i} - \sum_{i=1}^{N_R} n_{R_i}\mu_{R_i} \quad (2)$$

where the μ_{R_i} and μ_{P_i} are the chemical potentials of the reactants and products and N_R and N_P are the number of reagent and product species respectively. Making use of the relationships

$$\mu_{R_i} = \mu^o_{R_i} + RT \ln[R_i] \quad (3)$$

and

$$\mu_{P_i} = \mu^o_{P_i} + RT \ln[P_i] \quad (4)$$

where the μ^o_P and μ^o_R are the standard-state free energies per mole of the reactants and products, we have

$$\Delta G = \Delta G^o + RT \ln \frac{[P_1]^{n_{P_1}}[P_2]^{n_{P_2}} \cdots}{[R_1]^{n_{R_1}}[R_2]^{n_{R_2}} \cdots} \quad (5)$$

ΔG^o is the free energy change of the reaction when all reagents and products are present at concentrations of one molar. At equilibrium, ΔG is equal to zero so that

$$\Delta G^o = -RT \ln\left[\frac{[P_1]^{n_{P_1}}[P_2]^{n_{P_2}} \cdots}{[R_1]^{n_{R_1}}[R_2]^{n_{R_2}} \cdots}\right]_{eq} \qquad (6)$$

The quantity in brackets in this equation is K_{eq}, the equilibrium constant for the reaction. The dependence of ΔG^o, and thus K_{eq}, on temperature and pressure is derived by recalling that

$$\Delta G = \Delta H - T\Delta S + S\Delta T = \Delta E + V\Delta P + P\Delta V - T\Delta S - S\Delta T \qquad (7)$$

where ΔH, ΔS, ΔE, ΔV, ΔP, ΔT represent the changes in the enthalpy, entropy, internal energy, volume, pressure and temperature upon going from the reactants to the products. As biochemical reactions generally take place under conditions of constant pressure and temperature, the quantities ΔT and ΔP are equal to zero and

$$\Delta G = \Delta E + P\Delta V - T\Delta S \qquad (8)$$

so that

$$\frac{d(\ln K_{eq})}{dP} = \frac{d(-\frac{\Delta G^o}{RT})}{dP} = -\frac{\Delta V^o}{RT} \qquad (9)$$

If, for instance, the products of the reaction occupy a larger volume than the reactants,

ΔV^o is positive and an increase in pressure, dP, will cause $\ln(K_{eq})$ to decrease by $dP \times \Delta V^o/RT$. This is in accord with LeChatelier's principle, which states that a system at equilibrium subjected to a perturbation will act to reduce the effect of the perturbant. A system subject to an increase in pressure will therefore act to decrease the quantity PV. Put simply, an increase in pressure will cause the equilibrium to shift toward the side that occupies the least volume.

If we now consider a simple association-dissociation reaction between two proteins A and B:

$$AB \rightleftharpoons A + B \tag{10}$$

at equilbrium

$$\frac{[A][B]}{[AB]} = K_{eq} = K_d = e^{\frac{-1}{RT}(\Delta E^o + P\Delta V^o - T\Delta S^o)} \tag{11}$$

so

$$\frac{d(\ln K_d)}{dP} = -\frac{\Delta V^o}{RT} \tag{12}$$

where ΔV^o is now the difference betweeen the partial molar volumes of the dissociated proteins and the complex. It should be clear that the application of pressure will shift the equilibria toward either the complex or the dissociated proteins depending on which has the smaller partial molar volume.

The vast majority of protein-protein associations characterized to date are reversed by increasing pressure in the range of 100 bar to 2.5 kbar. Protein-protein associations

are therefore accompanied by positive changes in volume. The basis for the increase in volume upon association is best understood by considering the classical hierarchy of bonds that stabilize proteins and protein-protein interactions.

Covalent Bonds.

To a first approximation covalent bond energies are well represented by the Born repulsion function.

$$\Delta E(r) = Br^{-13} - Cr^{-6} \qquad (13)$$

In this equation r is the interatomic distance and B and C are constants specific to the atoms involved. As shown in figure 2-1, this equation is characterized by a high energy barrier at bond lengths less than that of the energy minimum. For this reason covalent bonds are essentially incompressible over the range of pressures in which protein-protein complexes are known to be affected (Benson and Drickamer, 1957). With the exceptions of cis-trans or boat-chair isomerizations, bond angles are likewise unaffected by pressure in this range (Weber and Drickamer, 1983). Over this range of pressures, the covalent architecture of a protein may therefore be considered incompressible.

Electrostatic Interactions.

The breaking of a salt bridge results in the exposure of the charged groups of the ion pair to water. This is accompanied by close packing of water dipoles around the charged groups and therefore results in a decrease in volume. Experiments with model

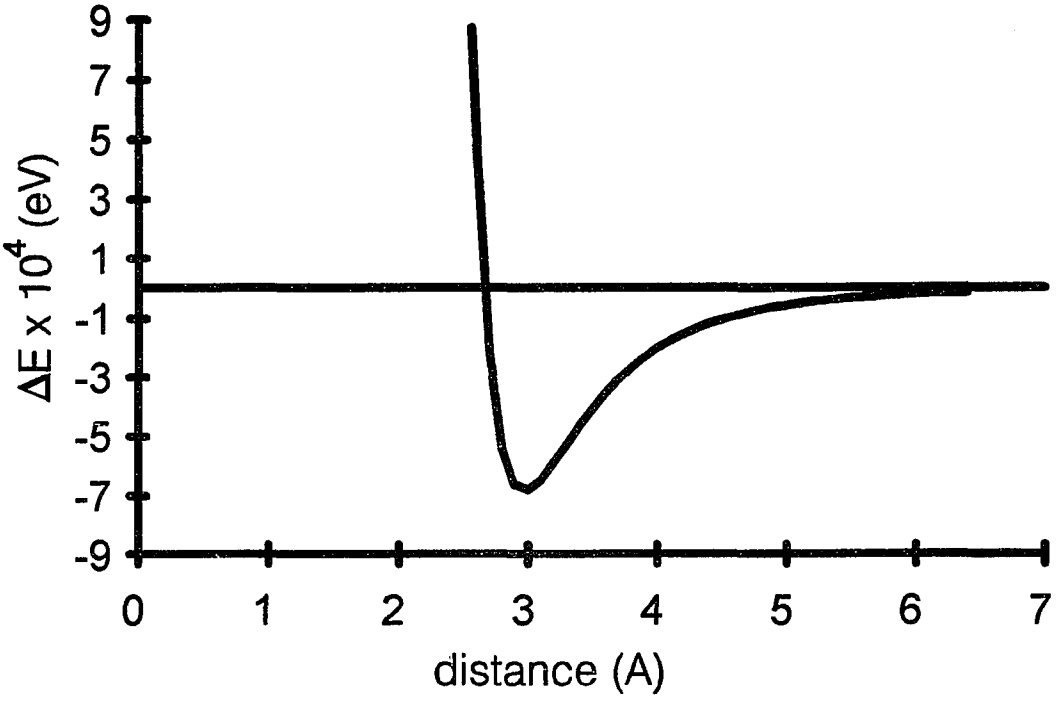

Figure 2-1. The Born repulsion function.

compounds suggest that the volume decrease associated with breaking an ionic bond, known as electrostriction, is on the order of 20 ml/mole. From equation 12 we can calculate that a single ionic pair can cause the K_d to double at 1 kbar. Ionic interactions would therefore be expected to be a major determinant of the behavior of associating protein systems under conditions of increased pressure.

Hydrogen bonds.

Experiments with model systems indicate that a small negative volume change is associated with the formation of a hydrogen bond. An often quoted example is the self-association of phenol in CCl_4. The ΔV for this association is -2.3 ml/mol. In associating protein systems, however, the breaking of hydrogen bonds at the protein-protein interface is expected to be acccompanied by the formation of roughly equal or perhaps slightly higher number of hydrogen bonds between the newly exposed protein surfaces and water (Heremans, 1982). For this reason, hydrogen bonding is not considered to play a major part in the behavior of protein system under conditions of high pressure.

Hydrophobic Interactions.

The effect of hydrophobic interactions on the behavior of proteins subjected to pressure seems to have been an issue of some controversy in the early treatments of the subject (see reviews by Morild, 1981; Heremans, 1982; Weber and Drickamer, 1983). It is clear from studies with model compounds that the partial molar volume of organic compounds is smaller when these compounds are transferred from a nonpolar solvent to water. It was inferred from these studies that association of hydrophobic groups in water

would lead to a positive volume change as dipole-induced dipole interactions with water were replaced by nonpolar interactions between these groups. However, a 1974 paper by Weber *et al.* (1974) showed that the self-association of aromatic compounds is enhanced by increased pressure, and cast doubt on the relevance of transfer studies to studies of dilute solutions of hydrophobic compounds in water. The current consensus theory divides effects of hydrophobic interactions on ΔV into effects due to hydrophobic solvation and effects due to solvent-induced hydrophobic interactions. Hydrophobic solvation effects include the dense packing of water around an apolar molecule and are well modeled by transfer studies. Hydrophobic solvation leads to the expected increase in ΔV for the association of apolar molecules. Solvent-induced hydrophobic interactions include, for instance, the ring-stacking behavior observed for solutions of aromatic molecules under pressure. Effects due to solvent-induced hydrophobic interactions are expected to be minimal for aliphatic compounds. Thus the association of aliphatic groups is decreased by an increase in pressure while the association of aromatic groups may be enhanced.

The contribution of these hydrophobic effects to the overall behavior of associating protein systems subjected to pressure is difficult to determine but is probably small. The interfacial region between two proteins is unlikely to be as hydrophobic as pure organic solvent and contributions due to aromatic-type and aliphatic-type interactions would be expected to balance out.

The effect of dead spaces.

As noted above, the lengths and angles of the covalent bonds responsible for determining the overall structure of a protein are unlikely to be changed at pressures at which protein-protein dissociation is typically observed. The conformational constraints imposed by these covalent bonds, however, have an indirect effect on the behavior of associating protein systems subjected to pressure, which cannot be understood by studying small model compunds. These conformational constraints restrict the amino acid residues at protein interfaces from packing against each other as well as they would pack against water. For this reason interactions between proteins result in the creation of small spaces at interfacial areas that cannot be filled by solvent. These unfilled 'dead spaces' will disappear upon dissociation of the interacting proteins as solvent is allowed to pack around the residues that made up the former contact surfaces. The formation of dead spaces upon protein-protein association will cause an increase in the ΔV of association and will therefore increase the tendency of the proteins to be dissociated by pressure. Although the contribution of dead space to the overall ΔV of association is expected to be proportional to protein-protein contact area, the proportionality constant is difficult to obtain experimentally as it would be difficult to separate the effect of dead spaces from the other effects outlined above. (Although it seems likely that an estimate of dead space volume could be obtained from a study of the crystal structures of protein complexes.) The dominance of this effect in determining the ΔV of association can, however, be inferred from the observation that an increase in dissociation with increasing pressure seems to be the rule for a wide variety of proteins studied under a variety of different

solvent conditions. Furthermore, the variability of ΔV from system to system seems to be small, with the majority of ΔV's measured falling in the range from 60 to 200 mL mol^{-1}. This consistency would not be expected if the ΔV of association were determined solely by the number and type of bonds at the protein-protein interface.

In summary, the terms which contribute to the positive ΔV observed for the formation of most protein complexes are 1) a contribution of approximately 20 ml mol^{-1} for each salt bridge formed, 2) a small but positive contribution due to difference in the total number of hydrogen bonds formed with solvent versus those formed at protein-protein interface, 3) an unknown but probably small positive contribution due to a decrease in the number of dipole-induced dipole interactions at the protein interface versus those formed with water, and 4) an unknown but probably large contribution due to formation of "dead spaces" upon association. Each of these effects results from the interaction of protein surfaces with solvent (water). None of these effects are derivable from consideration of proteins in vacuo. Thus, as with the more widely studied contributors to the free energy of association, enthalpy and entropy, the volume change of association is a property of the entire system: protein and solvent.

Apparatus for High Pressure Dissociation Experiments.

The apparatus used for the high pressure dissociation studies performed in chapter 3 is diagramed in figure 2-2. This apparatus closely resembles that described by Paladini and Weber (Paladini and Weber, 1980) and the reader is referred to that paper for a detailed description of the construction of the high pressure bomb. The sample to be

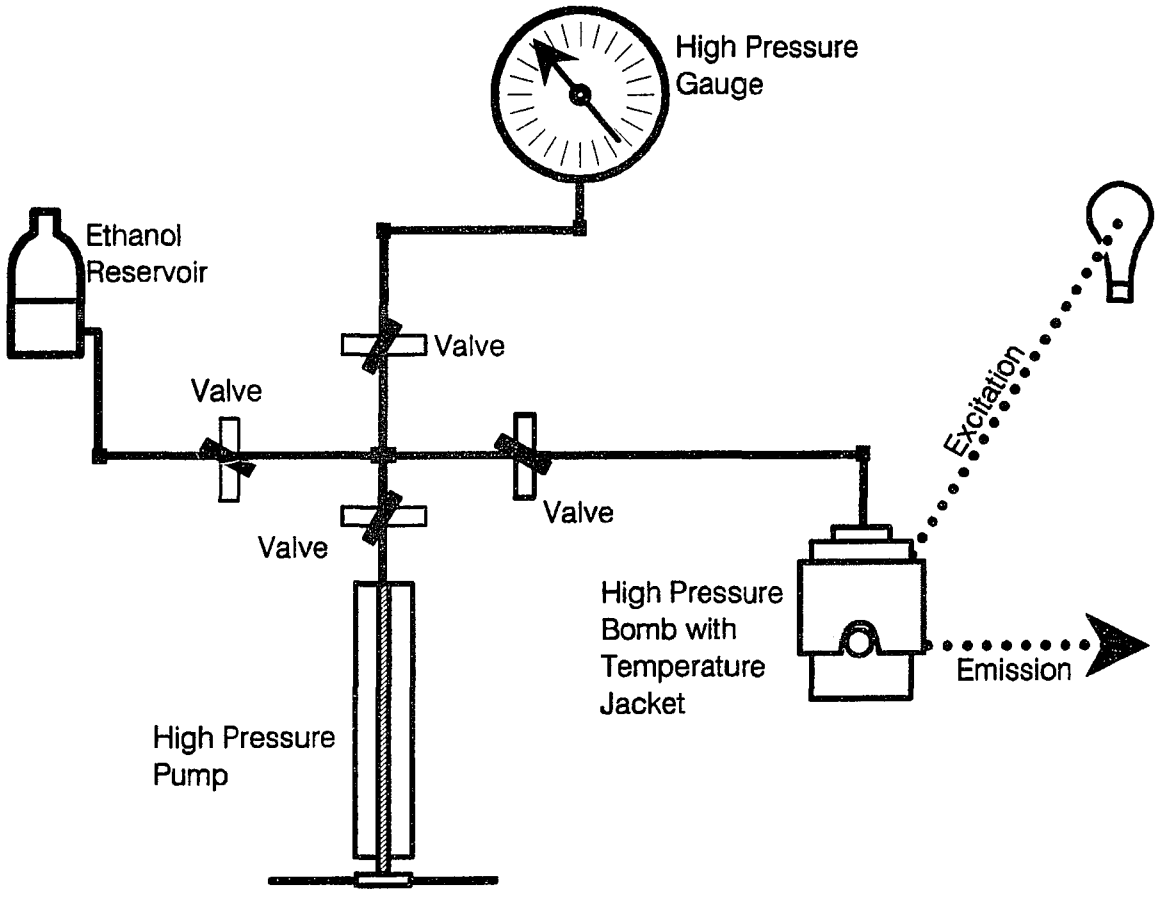

Figure 2-2. Schematic diagram of the high-pressure spectroscopy apparatus.

studied is placed in a bottle-shaped cuvette made of fused quartz and is capped with a small piece of polyethylene tubing which has been sealed at one end. Sample volume is approximately 1 mL. The cuvette is placed in the high pressure bomb and the bomb is filled with ethanol. The flexible polyethylene cap isolates the sample from the ethanol but allows pressure to be transduced from the ethanol to the sample. The refractive index of the ethanol closely matches that of the cuvette so that the cuvette boundaries are effectively invisible. The sample may be observed spectroscopically via four fused quartz windows placed at right angles around the bomb. The fused quartz used (Ultrasil T-19, Karl Lambrecht Corp, Chicago) has good ultraviolet light transmittance properties and shows lower pressure-dependent scrambling of polarized light than alternatives such as sapphire (see below). Pressure is generated against the ethanol using a manually-turned screw pump (High Pressure Equipment, Erie PA) and is monitored by a Bourdon type gauge (Heise, Newtown, CT). Connections between the pump, gauge and bomb are laid out so that any component may be isolated and checked for leaks. A temperature jacket connected to a circulating water bath is placed around the bomb to maintain temperature to within ±0.2° C.

Analysis of pressure dissociation curves.

In a typical pressure dissociation experiment, a spectroscopic observable proportional to α, the percent of complexed protein, is measured over a range of pressures starting at atmospheric pressure (~1 bar). For a heterodimeric association such as described by equation 10

$$\alpha = \frac{[AB]}{A_0} \tag{14}$$

For known values of A_o , B_o, and $K_{d,P}$, the dissociation constant at a given pressure, α_P may be calculated from the equation

$$\alpha_P = (\frac{1}{2A_o})[(K_{d,P}+A_0+B_0)-\sqrt{((K_{d,P}+A_0+B_0)^2-4A_0B_0)}] \tag{15}$$

Integration of equation 12 leads to an expression for $K_{d,P}$ in terms of ΔV, P, and $K_{d,atm}$

$$K_{d,P} = e^{(\ln K_{d,atm} - P\Delta V)} \tag{16}$$

Combination of equations 15 and 16 yields a cumbersome expression for α_P, in terms of ΔV, P, and $K_{d,atm}$. For this reason, pressure dissociation data is often presented as a plot of $\ln(K_{d,P})$ versus P. This plot yields a straight line with a slope of $\Delta V/RT$ and an intercept equal to $\ln(K_{d,atm})$. The availability of a wide variety of flexible data analysis and graphics software packages makes linearization unnecessary. Furthermore, regression analysis is best performed using untransformed data so that error bars and, by extension, weighting factors may be determined without resorting to complicated propagation of errors analysis.

Figure 2-3 shows the pressure dissociation curves expected for a heterodimeric.

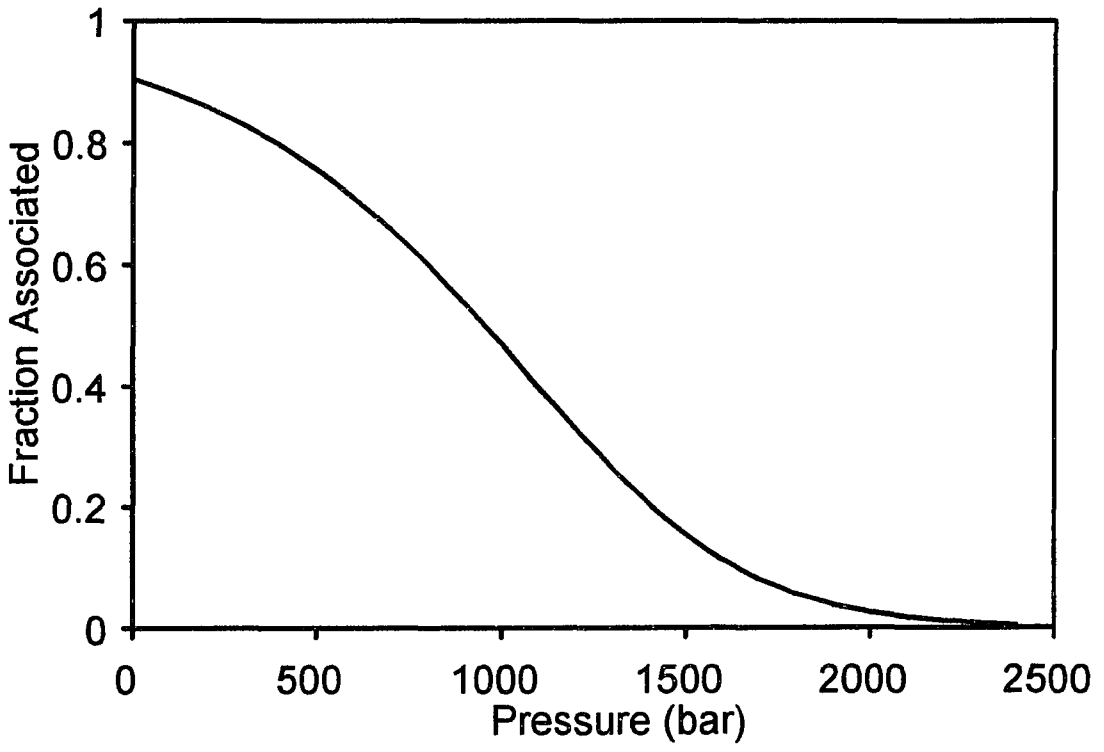

Figure 2-3. Pressure dissociation curve for a heterodimeric association reaction. $K_{d,atm}$ = 1 atm, $A_o = B_o$ = 100 nM, and ΔV = 100 mL mol^{-1}

association for which $K_{d,atm}$ = 1 nM, $A_o = B_o$ = 100 nM, and ΔV = 100 mL mol^{-1}. α decreases from 0.9 at atmospheric pressure to nearly 0 at 2.4 kbar, the maximum pressure achieved. The maximum α observed is determined solely by A_o, B_o and $K_{d,atm}$, whereas α at any given pressure is a function of all of these and ΔV.

Figure 2-4 demonstrates the effect of ΔV on a graph of α versus P. $K_{d,atm}$, A_o, and B_o have been held fixed at 1, 100, and 100 nM, respectively. Curves are shown for ΔV = 60, 80, 100 and 120 ml mol^{-1}. It can be seen that while ΔV has no effect on the value of α at atmospheric pressure it has a strong effect on the rate at which α decreases with pressure. Note that while the curves for the 80, 100 and 120 mL mol^{-1} simulations clearly show plateaus at low and high pressures, no plateau is seen at 2400 bar for the simulation for which ΔV has been set to 60 ml mol^{-1}. In this situation the limiting value for the observable at complete dissociation cannot be determined from this experiment and must, if possible, be determined independently.

Figure 2-5 demonstrates the effect of $K_{d,atm}$ on a graph of α versus P. ΔV, A_o, and B_o have been held fixed at 100 ml mol^{-1}, 100 nM and 100 nM, respectively. Curves are shown for $K_{d,atm}$ = 40 pM, 200 pM, 1 nM, and 5 nM. It can be seen that $K_{d,atm}$ effects the both maximum and minimum α observable at this concentration over this range of pressures. Note, however, that the relatively small differences in α at atmospheric pressure ($0.05 \leq \alpha \leq 0.20$ for 40 pM $\leq K_{d,atm} \leq$ 5 nM) are greatly magnified at an intermediate pressure such as 1 kbar. This magnification is indicative of the ability of high pressure dissociation methods to resolve differences in 'tight' binding constants.

Figure 2-6 shows how the total protein concentration effects the graph of α versus

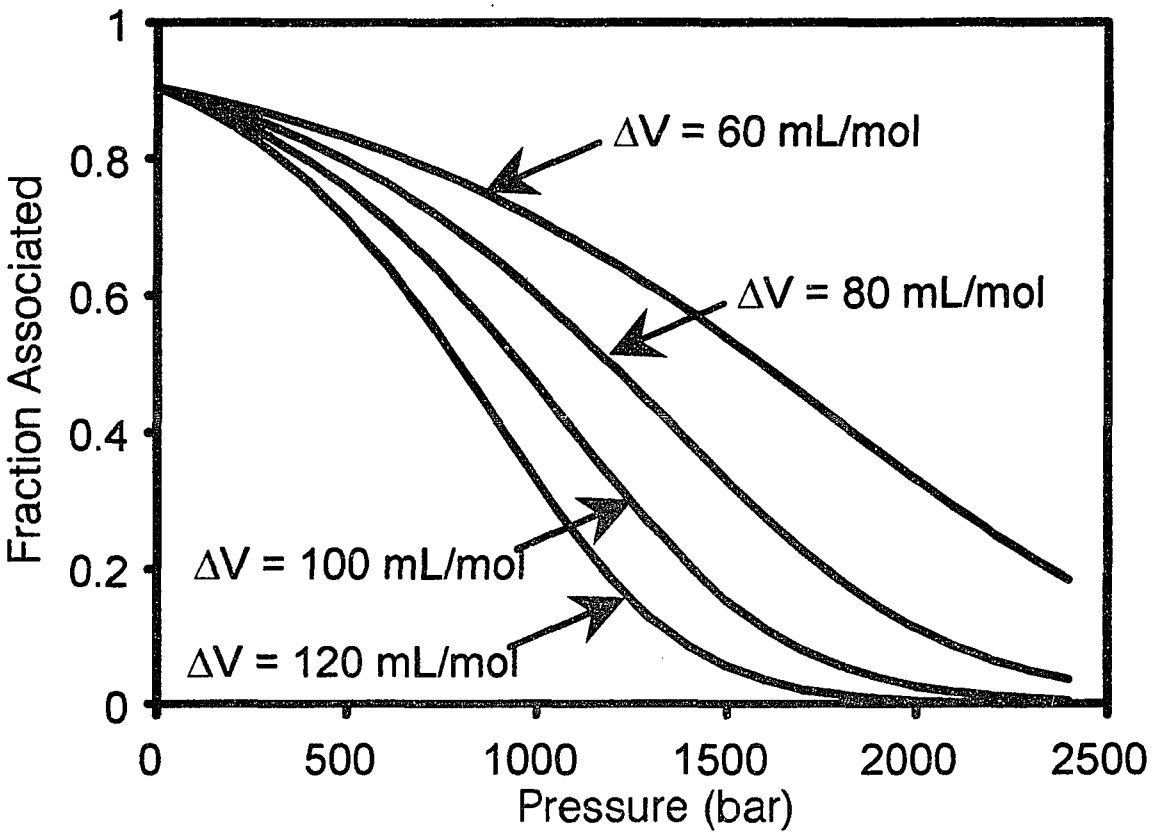

Figure 2-4. Effect of ΔV on a graph of α versus P. Kd,atm, Ao and Bo are 1, 100, and 100 nM for all curves. ΔV's are as indicated

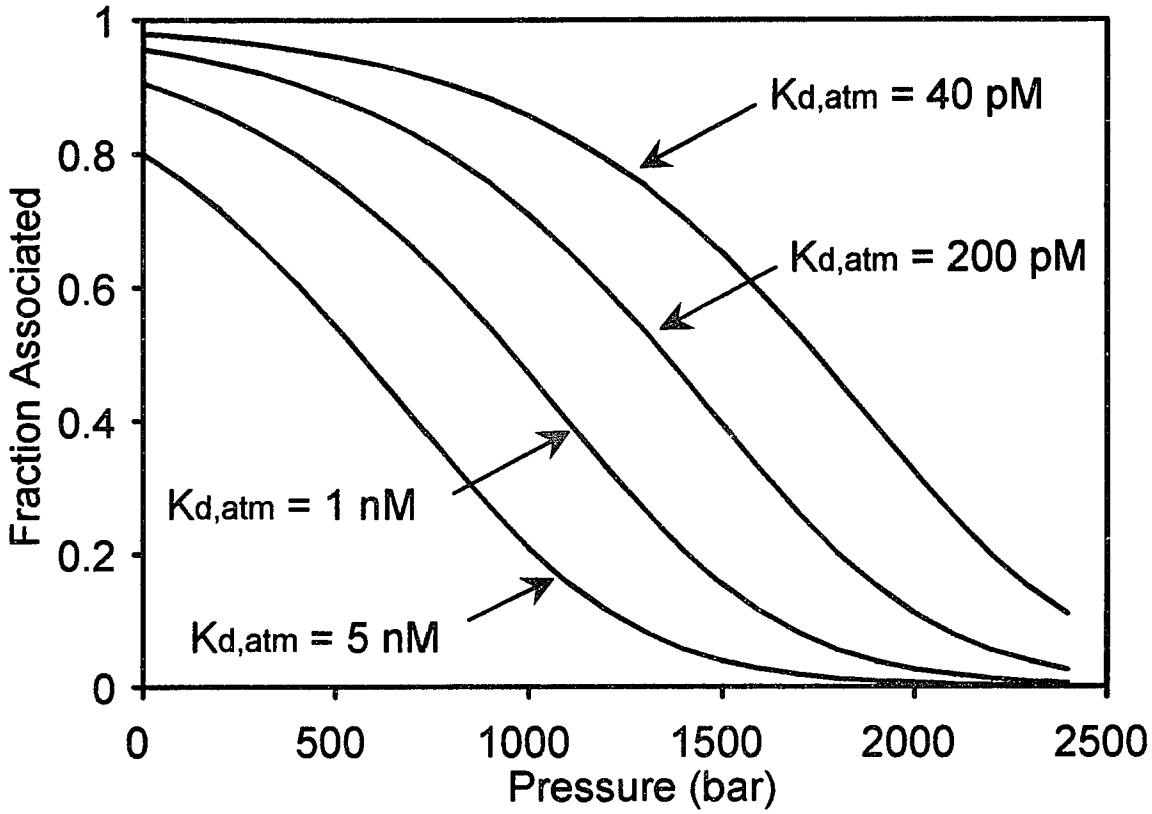

Figure 2-5. Effect of $K_{d,atm}$ on a graph of α versus P. ΔV, Ao and Bo are 100 mL mol^{-1}, 100 nM and 100 nM for all curves. $K_{d,atm}$'s are as indicated.

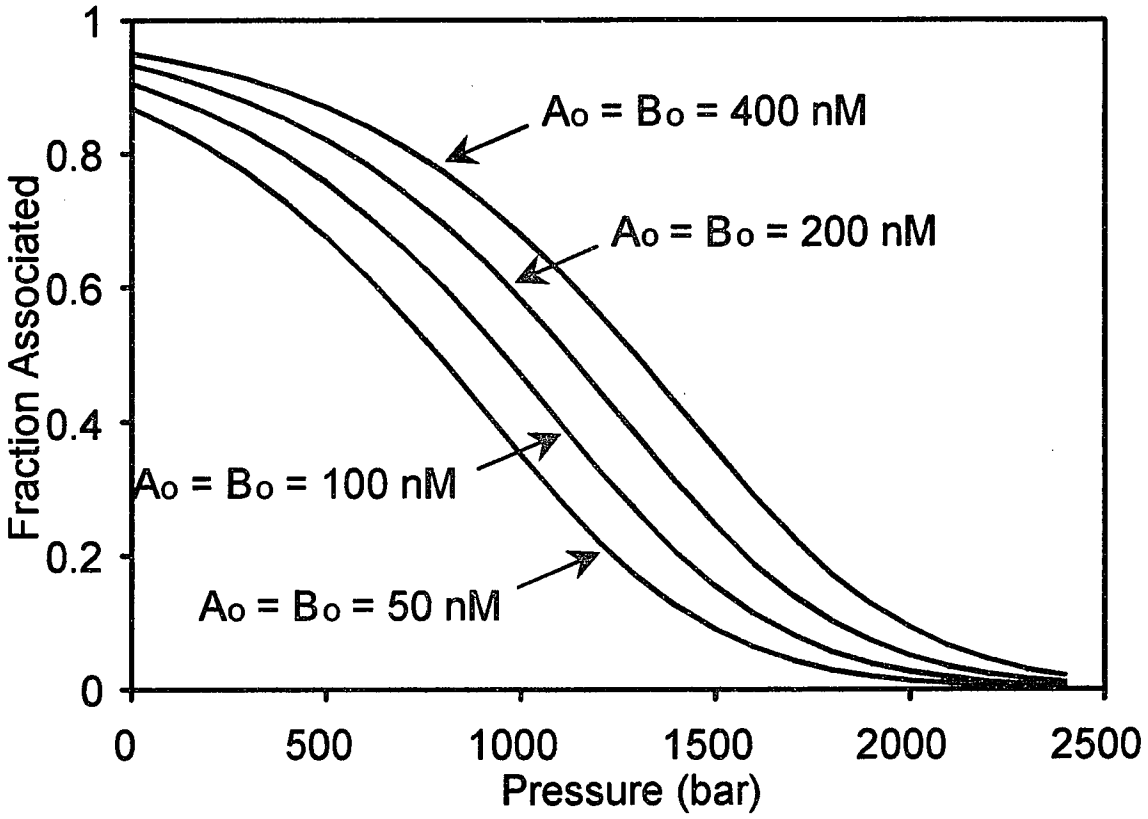

Figure 2-6. Effect of concentration on a graph of α versus P. ΔV and $K_{d,atm}$ are set at 100 mL mol^{-1} and 1 nM, respectively. A_o and B_o are equal with values as indicated..

P. In this figure, ΔV has been fixed at 100 ml mol^{-1}, and $K_{d,atm}$ has been fixed at 1 nM. Curves are shown for $A_o = B_o$ = 50, 100, 200, and 400 nM. It can be seen that total protein concentration effects the pressure dissociation curve in a manner similar to $K_{d,atm}$. This fact has two implications for the use of high pressure dissociation to determine $K_{d,atm}$. The first is that $K_{d,atm}$ can only be determined as accurately as the total protein concentration. This is, of course, true for any method of determining a dissociation constant. The second is that the assumption that equation 10 (or any other association model) accurately reflects the system can be checked by performing pressure dissociation experiments over a range of different total protein concentrations.

Under ideal conditions the concentration of protein in the sample may be chosen so that the protein is at least 90% associated at atmospheric pressure and is not more than 10% associated at the maximum pressure achievable. The maximum pressure achievable is generally limited to approximately 2500 bar when quartz windows are used in the high pressure bomb; thus it is not always possible to observe α over the complete 10% to 90% range. In this situation it is neccesary to determine the value of observable corresponding to α_{max} and α_{min} in a separate experiment.

Pressure Denaturation.

The types of bonds involved in stabilizing the structure of a protein are identical to those responsible for protein complex formation. Furthermore, the folding of a protein would be expected to create "dead spaces" in much the same way as they are created by

the formation of a protein complex. It seems reasonable then to assume that, in addition to dissociating protein complexes, pressure should also cause proteins to unfold. In fact, some of the earliest studies of the behavior of proteins at high pressure demonstrated that some type of unfolding does occur (see review by Weber and Drickamer, 1983), but generally at much higher pressures (> 4 kbar) than are known to cause protein complex dissociation. This apparent paradox can be resolved by examining the relationship between K_{eq} and α, the degree of unfolding, for a simple two state equilibrium between folded and unfolded forms of the protein.

$$A_{folded} \rightleftharpoons A_{unfolded}; \quad \alpha = \frac{[A_{folded}]}{A_0}; \quad K_{eq} = \frac{[A_{unfolded}]}{[A_{folded}]} = \frac{\alpha}{(1-\alpha)} \qquad (17)$$

K_{eq} and by extension, α, is independent of the total concentration of protein. The $P\Delta V$ energy required to shift the equilibrium towards unfolding cannot be lowered by lowering total protein concentration. Figure 2-6 demonstrates that concentration has a considerable effect on protein dimer formation.

Figure 2-7 illustrates this effect. This graph shows the pressure dissociation curve for a heterodimeric assocation alongside a pressure denaturation curve. The parameters used to generate the dissociation curve were $K_{d,atm}$ = 1 nM , ΔV = 100 mL mol^{-1}, and A_o = B_o = 100 nM. The parameters used to generate the denaturation curve were, ΔG = -10 kcal mol^{-1}, and ΔV = 100 ml mol^{-1}. The graph clearly shows that despite the fact that ΔV is the same for the two equilibria, and that the standard state free energy of folding is

smaller in magnitude than that of the association reaction, the concentration dependence of the association equilibria poises this equilibrium at the brink of dissociation at this concentration.

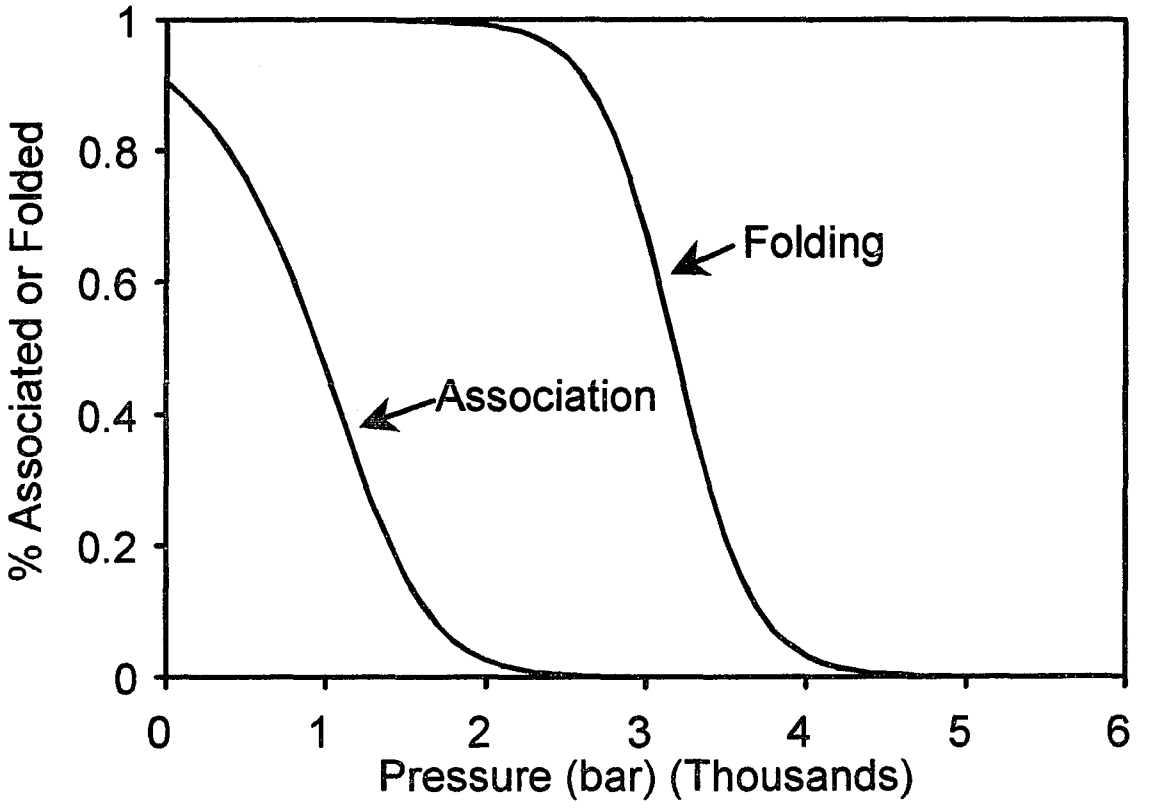

Figure 2-7. Comparison of pressure dissociation of a heterodimer and pressure denaturation curves. For the heterodimer dissociation ΔV =100 ml mol-1. Kd,atm = 1 nM, and Ao = Bo = 100 nM. For the pressure denaturation, the free energy of denaturation was set to -10 kcal mol-1.

References for Chapter 2

Benson, A.M., and Drickamer, H.G. (1957) *J Chem. Phys. 27*, 1164-1174

Deranleau, D. (1969)*J. Amer. Chem. Soc.*91, 4044-4049.

Heremans K. (1982) *Ann. Rev. Biophys. Bioeng.* 11, 1-21.

Morild, E. (1981) *Advances in Protein Chemistry* 34, 93-166.

Paladini, A. and Weber, G. (1983) *Methods in Enzymology* 53, 419-427.

Weber, G., and Drickamer, H.G., (1983) *Quart. Rev. Biophys.* 16, 89-112.

CHAPTER 3

TISSUE FACTOR AND ITS EXTRACELLULAR SOLUBLE DOMAIN: THE RELATIONSHIP BETWEEN INTERMOLECULAR ASSOCIATION WITH FACTOR VIIa AND ENZYMATIC ACTIVITY OF THE COMPLEX

from Waxman et al, 1992

INTRODUCTION

The complexation of factor VIIa (VIIa) with tissue factor (TF) is widely believed to be a critical step in the initiation of blood coagulation. As it occurs in nature, TF is a transmembrane glycoprotein consisting of an extracellular domain (residues 1-219), a single transmembrane domain (residues 220-242), and a cytoplasmic domain (residues 243-263) with a sequence that contains a half-cysteine residue thioesterified to palmitate or stearate (for review see Bach, 1988). When complexed with TF, the proteolytic activity of VIIa, a serine protease, towards its natural substrate, factor X (X), is increased by many orders of magnitude (Silverberg et al., 1977).

TF is frequently referred to as a "receptor" (Edgington et al., 1991), implying that docking of VIIa to transmembrane TF without concomitant conformational change in VIIa is sufficient to endow it with enhanced proteolytic activity. In this model, the interaction between VIIa and TF is passive, and the enhanced activity derives solely from facilitation of assembly of the cofactor:enzyme:substrate complex, TF:VIIa:X, on the membrane surface. However, detailed kinetic studies of the TF:VIIa complex indicate that TF is an essential enzyme activator (Nemerson & Gentry, 1986). This implies that structural alterations occur in VIIa upon formation of the binary complex with TF.

Studies of the TF:VIIa binding interaction are complicated by the requirement that full-length TF be reconstituted in phospholipid vesicles or solubilized in detergent. This makes the possible interactions of TF and VIIa which involve the lipid or detergent difficult to resolve from those due strictly to direct protein-protein interactions, and complicates the thermodynamic description of the TF:VIIa interaction. To resolve these

contributions, we have prepared a soluble TF (TF_{1-218}; sTF) which lacks the transmembrane and cytoplasmic domains.

In the presence of exogenous vesicles consisting of phosphatidylserine and phosphatidyl-choline (30/70, w/w), the sTF:VIIa complex has about 4% of the activity of TF_{1-263}:VIIa. In this communication, we examine and compare the nature of the complex formed by VIIa and sTF with that formed with full-length TF (TF_{1-263}) inserted into phosphatidylcholine vesicles. We show that the reduced activity of sTF relative to full-length TF does not result from impaired VIIa-binding, as the assays were performed using conditions that would result in >90% of the TF molecules being complexed with VIIa. Furthermore, we have determined ΔG, the free energy of binding, and ΔV, the molar volume change, for association at 25° C of sTF or TF_{1-263} to VIIa. In the case of TF_{1-263}, the K_d is 7 pM; with sTF it is 500 pM. Further, when factor VIIa binds to TF_{1-263}, there is a volume increase of 117 mL mol^{-1}; with sTF the volume increase is 63 mL mol^{-1}. Thus, we have demonstrated that the two binary complexes are structurally different. We propose that it is this structural difference and not binding *per se* that is reflected in the differences in activity of sTF and TF_{1-263}.

EXPERIMENTAL PROCEDURES

Experimental Approach: Measurement of associations in the pM-to-nM concentration range under equilibrium conditions is technically difficult. Earlier studies measured the degree of dissociation by separation of free from bound VIIa by centrifugation, which is not an equilibrium technique. To overcome the inherent

difficulties in measuring tight binding, while still meeting the requirement of observing the system at equilibrium, we have utilized the techniques of high pressure dissociation and fluorescence anisotropy. Fluorescence anisotropy studies were performed using fluorescent-labelled VIIa covalently modified at its active site with dansyl-D-Phe-L-Phe-Arg-chloromethyl ketone (DF-VIIa).

Theoretical Considerations: The ability of pressure in the range of 0.1 to 3 kbar to dissociate protein complexes is well documented (Heremans, 1982; Weber & Drickamer, 1983). This effect can be understood by examining the thermodynamic expression for a simple dissociation $AB \rightleftharpoons A + B$. At equilibrium,

$$K_d = e^{[-\Delta G^o/RT]} = e^{[-(\Delta E^o + P\Delta V^o - T\Delta S^o)/RT]} \qquad (1)$$

where K_d is the equilibrium dissociation constant, and ΔG°, ΔE°, ΔV°, ΔS° are the standard changes in free energy, internal energy, volume, and entropy, respectively. Consequently, the application of pressure drives the equilibrium towards association or dissociation, whichever condition takes up the least volume, according to the relationship

$$\delta(\ln K_d)/\delta P = -\Delta V^o/RT\ . \qquad (2)$$

Interactions between proteins result in the creation of small spaces at interfacial areas that cannot easily be filled by solvent. Some of these unfilled volumes will disappear upon dissociation due to better packing of the solvent at the former contact surfaces. For this reason, protein-protein associations are generally characterized by positive volume changes and application of pressure shifts the binding equilibrium towards dissociation.

The interaction of VIIa with sTF and TF_{1-263} was investigated by observing the change in the steady-state fluorescence anisotropy of a dansyl probe covalently attached to the active site of VIIa (see below). The anisotropy, r, is given by

$$r = (I_{VV} - G \times I_{VH})/(I_{VV} + 2G \times I_{VH}), \quad (3)$$

where I_{VV} and I_{VH} are respectively, the emission intensities detected through vertical and horizontal polarizers, when vertical excitation is used and G is a factor which corrects for the transmissivity bias of the optics (Azumi & McGlynn, 1962; Paoletti & LePecq, 1969).

The anisotropy of light emitted by a collection of fluorophores free to rotate in solution is given by

$$r = r_o(1 + \tau/\phi)^{-1} \quad (4)$$

where τ is the fluorescence lifetime of the fluorophore and ϕ is the rotational correlation time, a measure of how fast the molecule is rotating. r_o is the limiting or "frozen" ansiotropy and accounts for depolarization due to factors other than molecular rotation. The rotational correlation time of a fluorescent molecule rigidly attached to a protein will depend on the solution viscosity, temperature, and the size and shape of the protein.

From these considerations, it is clear that the rotational correlation time of a protein in solution is likely to increase when the protein is in a macromolecular complex. In general, the anisotropy increase results primarily from a decrease in the global rotational motion of the protein and secondarily from a decrease in local motions due to binding interactions.

For a sample containing a mixture of free and bound labelled protein, the measured anisotropy, r_m, is

$$r_m = (r_f I_f + r_b I_b)/(I_f + I_b) , \quad (5)$$

where r_f, r_b, I_f, and I_b are the anisotropies and intensities of free and bound labelled protein. Defining Δr as the difference between the measured anisotropy and the anisotropy of the free protein ($\Delta r = r_m - r_f$), Δr_{max} as the difference between the anistropy of the bound protein and that of the free protein, and α as the degree of association we have

$$\alpha = (\Delta r/\Delta r_{max}) . \quad (6)$$

Measurement of anisotropy at high pressures is complicated by the pressure-dependent birefringence of the quartz windows. A method for correcting for this effect has been described by Paladini and Weber (1981). The correction factors involved, however, are difficult to obtain and may change as the windows age. We circumvented this by taking advantage of our ability to measure DF-VIIa anisotropy in the presence and absence of TF. At each pressure we determined $\Delta r_{pressure}$, the difference between the anisotropy of DF-VIIa alone and in the presence of an equimolar quantity of TF. Δr_{max} was determined from the titration of DF-VIIa with TF at atmospheric pressure. Because the absolute anisotropies of the TF:DF-VIIa complex and DF-VIIa alone are similar, their birefringence corrections will be essentially the same. In this situation, the correction to $\Delta r_{pressure}$ becomes negligible. We tested this approximation by comparing the observed maximum change in Δr for a titration at one atmosphere to the maximum change in Δr obtained from fitting the pressure dissociation data.

The data are analyzed according to equation 2. The quantity $\ln(K_d)$ is calculated from the fraction bound at each pressure and then plotted against pressure. The best

straight line through those data representing >10% dissociation is determined. The ordinate intercept of the line yields the K_d at atmospheric pressure, and its slope yields ΔV, the molar volume change for the association.

Apparatus for Atmospheric and High-Pressure Anisotropy Experiments: Fluorescence anisotropy measurements were performed on an SLM 4800 fluorometer modified in our laboratory for photon counting and computer control. The excitation monochromator bandwidth was 16 nm, and a 340 nm bandpass filter with a bandwidth of 10 nm was used to eliminate second order light. A polarization scrambler was used to make the vertical and horizontal intensities equal. The sample emission was detected through a 535 nm bandpass filter with a bandwidth of 10 nm. Measurements were repeated and averaged until the standard error of the anisotropy was 0.002 or smaller. Measured anisotropies were blank subtracted according to the equation

$$r_{corr} = (I_{sample} \times r_{sample} - I_{blank} \times r_{blank})/(I_{sample} - I_{blank}). \quad (7)$$

High pressure experiments were performed in a sample chamber (Paladini & Weber, 1981) built for us by the Physics Department machine shop at the University of Illinois, Urbana.

Equilibrium Ultracentrifugation Experiments: Sedimentation equilibrium studies of the sTF:VIIa complex were performed at 23° C in a Beckman Model E analytical ultracentrifuge equipped with an electronic speed control, RTIC temperature controller, Rayleigh interference optics, and a pulsed laser diode light source (670 nm). Data was acquired using a television-camera-based, on-line data acquisition and analysis system (Laue, 1981; Laue,1991). Samples were loaded into short column cells (0.7 mm)

(Yphantis, 1960) at several concentrations up to 1 mg/mL total protein. Data were collected at intervals after the estimated equilibrium time and tested for equilibrium by subtracting succesive scans (Yphantis, 1964). Blank correction was performed as described previously (Laue et al., 1984). The data from experiments at all concentrations were analyzed globally according to a model for an associating heterodimer (Luckow et al., 1989; Olsen et al., 1991) using the nonlinear least squares analysis package NONLIN (Johnson et al., 1981).

Proteins: Human recombinant VIIa, used for the dissociation studies, was a generous gift of Dr. Ulla Hedner, Novo Nordisk, Copenhagen. For activity assays, factors X and VIIa were purified from human plasma by the methods of Miletich et al. (1981) and Broze and Majeris (1980), respectively. The active site probe, dansyl-FFRcK, was prepared by reacting dansyl chloride (Sigma Chemical Co., St.Louis) with D-Phe-L-Phe-Arg-chloromethyl ketone (FFRcK) (Calbiochem, La Jolla) (C. Kettner, personal communication). VIIa was active-site labelled using 10μM dansyl-FFRcK in 50 mM Tris Buffer (pH 7.5, 0.1M NaCl). The extent of reaction with VIIa was assessed by measurement of coagulant activity in a two-stage assay (Bach et al.,1981). The reaction was complete after 3 h. DF-VIIa was separated from reagents on a G-15 Sephadex column. Incorporation of the dansyl label was determined by absorbance spectroscopy using molar extinctions of 58,400 $M^{-1}cm^{-1}$ at 280 nm for human VIIa and 1580 and 3940 $M^{-1}cm^{-1}$ at 280 and 340 nm for the dansyl group[1]. The labelling ratio observed was 1

[1]The extinction of human VIIa at 280 nm was based on the number of tryptophan and trysosine residues in recombinant VIIa (Thims et al., 1988) using average extinction coefficients for tryptophan (5,500 $M^{-1}cm^{-1}$) and tyrosine (1,200 $M^{-1}cm^{-1}$) residues in a protein

mole dansyl to 1 mole VIIa when VIIa was fully inhibited. An SDS gel run under reducing conditions showed that the fluorescent label was bound exclusively to the heavy chain of VIIa.

Recombinant human tissue factor (TF_{1-263}), with Cys_{245} replaced by Ser, was a generous gift of Dr. G. Vehar and Dr. D. Higgins, Genentech Inc, South San Francisco. TF_{1-263} was reconstituted into egg lecithin vesicles (Avanti, Alabaster, AL) by the procedure of Mimms et al. (1981). The lipid:protein molar ratio was 5,000:1. The activity of this protein is identical with that of native TF purified from human brain (see Bach, 1988).

Cloning and Expression of sTF: The soluble extracellular domain of TF (TF_{1-218}; sTF) was obtained by recombinant DNA techniques, the details of which will be reported elsewhere. Briefly, to prepare the expression vector containing the extracellular domain of the human TF structural gene, a 2147 bp DNA insert comprising the human TF coding region was obtained from a λgt11 recombinant phage (Spicer et al., 1987). This DNA insert was transfered first into plasmid pUC19 (Messing, 1983), and then into the replicative form of phage mp 19 (Yanis-Perron et al., 1985) to provide the ssDNA for oligonucleotide-directed mutagenesis. Thus, the TF coding sequence was truncated to include only the extracellular domain. For expression and export of sTF, this DNA fragment was positioned just 3' to a segment of DNA encoding the bacteriophage M13 gene VIII leader sequence and its corresponding ribosome binding site. This insert was

---

(Wetlaufer, 1962). The extinction of DF-VIIa was calculated using the extinction coefficients for ϵ-dansyl-lysine in water (J.B.A. Ross, unpublished data) and our calculated value for the extinction of VIIa at 280 nm, assuming additivity of the absorptions.

placed downstream from the *ptac* promoter in a plasmid that allowed expression of sTF in BL-21(DE3) *E. coli* cells after induction with isopropylthiogalactoside. After maintaining the cells at 25° C for 24 h, the media (6 L) was clarified and concentrated to about 300 mL.

Purification of sTF: The concentrated media was centrifuged at 12800 G for 1 h, $(NH_4)_2SO_4$ was added to the supernatant to 25% saturation; the precipitate was pelleted after 1 h, and the supernatant was brought to 65% saturation. After 1 h, the resulting precipitate was pelleted and dissolved in 50 mL of 25 mM sodium acetate buffer, pH 5.2. This solution was dialyzed against the buffer (2 × 2 L; eight h), and clarified by centrifugation. The supernatant was applied to a 75 mL S-Sepharose column, equilibrated with the buffer. The column was first washed with 250 mL of the same buffer and then the protein was eluted with a 500 mL linear gradient of NaCl (0 to 0.5M). sTF eluted at 160-208 mL. Following dialysis *versus* 25 mM Tris-Cl, pH 7.5 containing 0.2 mM EDTA (2 × 2 L, overnight), the sample was applied to 75 mL Q-Sepharose column equilibrated with this buffer. The column was washed with 250 mL of the same buffer; the proteins were then eluted with a 500 mL-linear gradient of NaCl (0 to 0.4 M). sTF eluted at 186-240 mL. The purity of the fractions was determined by SDS PAGE, and the fractions containing the homogeneous protein were pooled and concentrated. The typical yield was 15 mg of sTF from six liters of culture medium. The authenticiy of the expressed protein was established by amino acid composition, NH_2-terminal sequence analysis (10 residues), and by carboxypeptidase P digestion. The amino terminal sequence was that expected for human TF, and the carboxyl terminal digestion yielded

exclusively Arg (residue 218) rather than with the expected Glu, indicating that a single residue was removed by *E. coli* proteases. sTF concentrations were determined from the absorbance at 280 nM using an $A_1^{1\%}{}_{cm}$ of 14.9.

Assay of TF and sTF: TF was assayed by adding an appropriate amount of TF to a solution of VIIa (10 nM), X (250 nM) and Ca^{2+} (5 mM), in 10 mM Hepes, 0.14 M NaCl, 0.1% BSA, pH 7.5. The concentration of X was determined using an $A_1^{1\%}{}_{cm}$ of 11.6 (Di Scipio, et al., 1977). At intervals, 25 μL aliquots were withdrawn and added to 125 μL 50 mM EDTA, 0.05% BSA, pH 7.5. Spectrozyme Xa (American Diagnostica, Greenwich CT) was added to a final concentration 0.5 mM. The change in absorbance at 405 nm was monitored continuously for 10 min. Slopes were calculated from a least squares fit to the data. sTF was assayed in an identical manner except that the incubation mixture contained 10 μM PS/PC (30/70, w/w).

RESULTS

Comparison of the activities of sTF and TF_{1-263} The activities of sTF and TF_{1-263} reconstituted in PS/PC (30/70, w/w) vesicles were compared over a range of concentrations between 0.1 and 1 nM for sTF and between 0.01 and 0.1 nM for TF_{1-263}. These assays were performed in the presence of 10 nM VIIa and 250 nM X. Whereas sTF was found to be inactive in the absence of lipid, it exhibited activity in the presence of 10 μM PS/PC vesicles, corresponding to the lipid concentration when TF_{1-263} was present at 133 pM. Under these conditions, the activities were directly proportional to TF concentration and the ratio of activity of TF_{1-263}:VIIa to that of sTF:VIIa was approximately 25:1, assuming random orientation of TF_{1-263} in the vesicles (Bach, et al.,

1986). To determine whether the decreased activity of sTF:VIIa results from an altered interaction of sTF with VIIa, we compared the stoichiometry and dissociation constants for the sTF:VIIa association using ultracentrifugation and fluorescence anisotropy.

Ultracentrifugation Studies: Analysis of the equilibrium ultracentrifuge data shows that sTF and VIIa have molecular weights of 27,700 and 49,000, respectively. Neither protein shows a tendency towards reversible self-association at the concentrations examined. Analysis of the data obtained from studying an equimolar mixture of sTF and VIIa indicate that they form a complex with a molecular weight of 73,800, indicating a one-to-one stoichiometry. Analysis of the fringe displacement data according to a heterodimeric association model yielded an upper limit of 1 nM for the K_d. Determination of the K_d to greater accuracy and precision requires a more sensitive approach.

Fluorescence Anisotropy Studies: Titration experiments at atmospheric pressure were performed by the addition of concentrated aliquots of sTF or TF_{1-263} reconstituted in PC vesicles to samples containing 60 nM DF-VIIa in 50 mM Tris buffer, pH 7.5, 0.1 M NaCl, 5mM $CaCl_2$, and 0.1 mg/mL ovalbumin. The sample was maintained at 25±0.1° C. The results are shown in Figure 3-1. The graphs for both sTF and TF_{1-263} titrations show a linear increase in anisotropy up to approximately equimolar concentrations of TF followed by a sharp break, indicative of tight binding and saturation. An upper limit of approximately 1 nM for the K_d's for both sTF and TF_{1-263} with DF-VIIa was established by nonlinear least square fitting of these data to a bimolecular association model. The maximum change in anisotropy observed for association of TF_{1-263} and DF-VIIa was 0.027

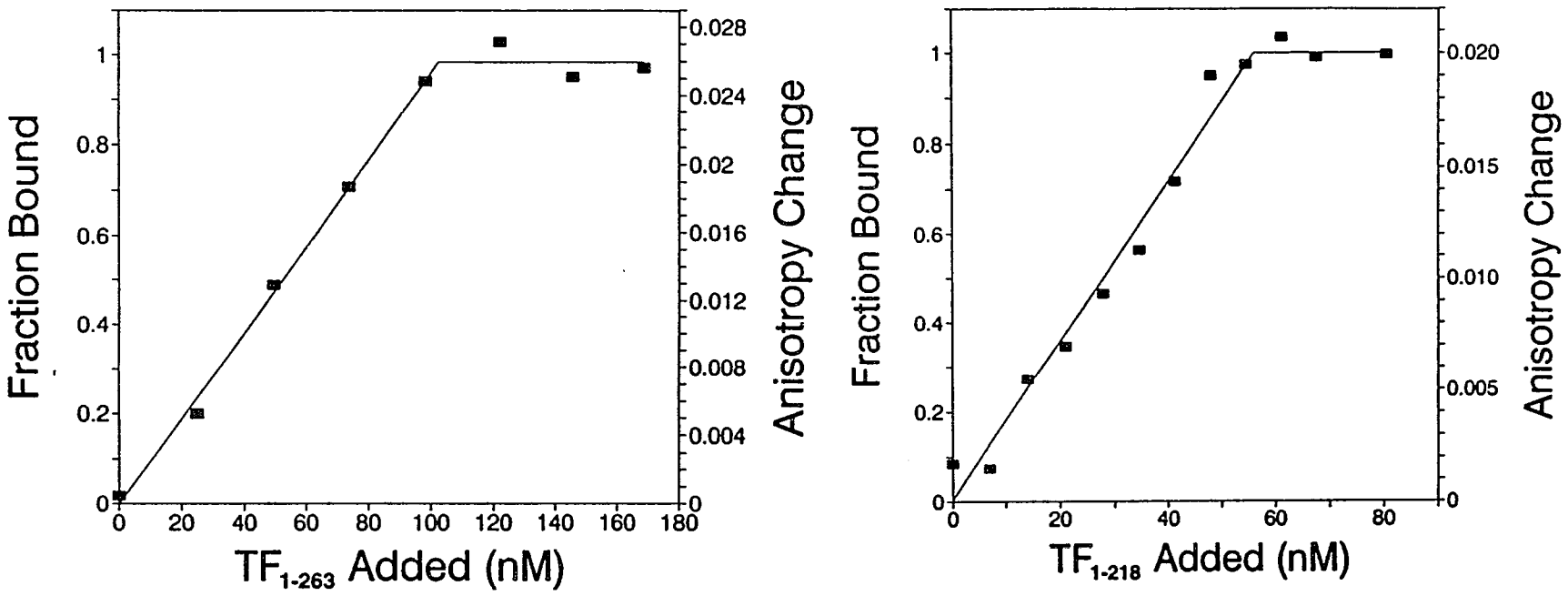

Figure 3-1. *Fluorescence anisotropy titration of DF-VIIa with sTF and TF_{1-263}:* See Results for conditions. The solid line in the left panel (sTF) and in the right panel (TF_{1-263}) represents the theoretical curve for a site titration. Examination of the residuals for fitting the data to a bimolecular association gave an *upper limit* of 1 nM for the $\mathbf{K_d}$ in each case.

while that observed for the association of sTF and DF-VIIa was 0.020. The most likely explanation for this difference is the dissimilarity in size of the membrane-bound and soluble complexes.

The pressure dependence of the anisotropy change of 100 nM DF-VIIa in the presence of either 100 nM sTF or TF_{1-263} is shown in Figure 3-2. The solid lines represent the best fits to the data. For TF_{1-263}, the free energy, ΔG, for complex formation is -15.1±0.3 kcal mol^{-1}. This ΔG corresponds to a K_d of 7.3 pM. The ΔV for the association is 117±9 mL mol^{-1}. By contrast, for sTF, ΔG is -12.5±0.1 kcal mol^{-1}, corresponding to a K_d of 0.59 nM. The ΔV for this association was 63±4 mL mol^{-1}.

The maximum anisotropy change used to determine these thermodynamic parameters was obtained from the titrations of DF-VIIa carried out at one atmosphere. Other values for Δr_{max} were evaluated for their ability to fit the data. For TF_{1-263}, any change in the value for Δr_{max} decreased the goodness of fit as measured by the residuals. This is strong evidence that our procedure for correcting for the birefringence-induced decrease in anisotropy as a function of pressure is correct. For sTF, Δr_{max} could not be fit for a unique value as the full dissociation curve was not achieved over a range from 1 bar to 2.4 kbar. Whereas 95% dissociation was observed for TF_{1-263} at 2.4 kbar, 80% dissociation was observed for sTF. Larger values of Δr_{max} could fit the data while smaller values resulted in statistically worse fits. However, it must be emphasized that the Δr_{max} determined by the value obtained from the titration at one atmosphere is an *upper limit*. The birefringence effects depolarize the emission driving all anisotropies towards zero. Values of Δr_{max} larger than that obtained at one atmosphere pressure are therefore

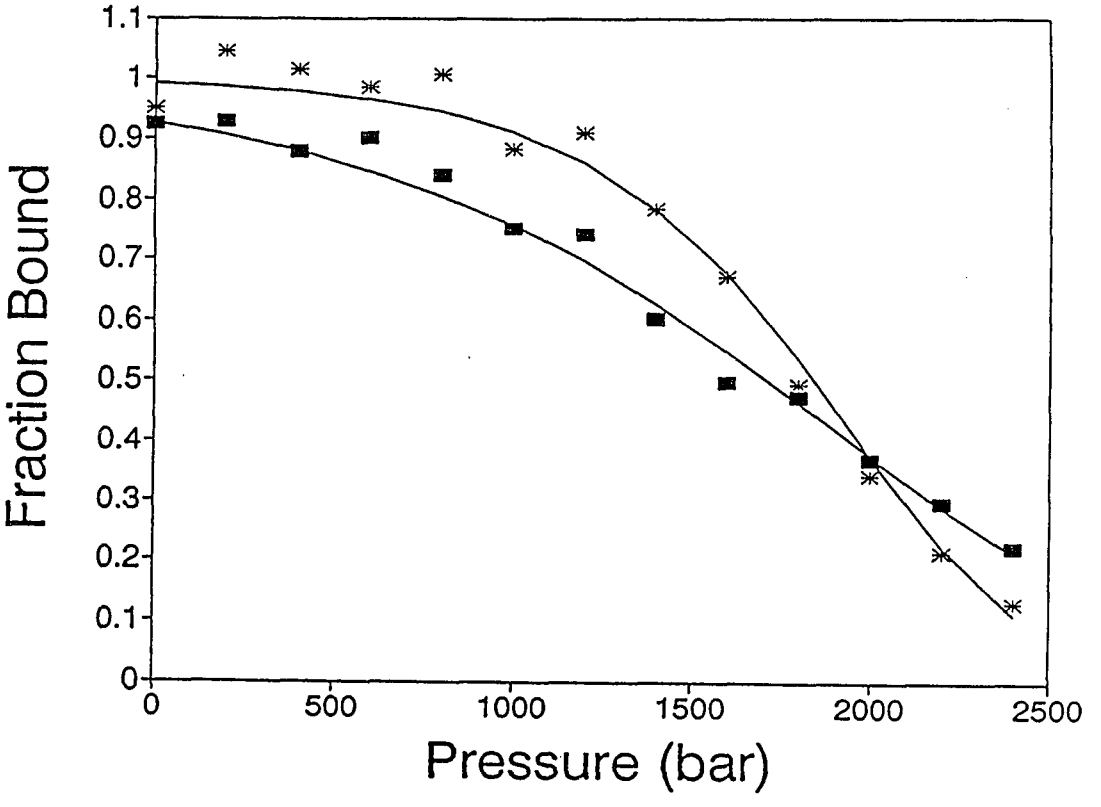

Figure 3-2. *Pressure dissociation of sTF:DF-VIIa and TF_{1-263}:DF-VIIa complexes:* Data for sTF:DF-VIIa(■) and TF_{1-263}:DF-VIIa (*) plotted as fraction bound *versus* pressure. The solid line represents the best fit theoretical curve calculated as described in *Theoretical considerations.*

physically unreasonable. Thus, the pressure data can be interpreted unambiguously.

Titration of VIIa with sTF: As yet another way of estimating the association of sTF and VIIa, we measured the ability of the complex to activate factor X, making the assumption that the fractional occupancy of VIIa with sTF is proportional to the reaction velocity. Because no reaction is observed in the absence of lipids, we allowed sTF, VIIa, X and Ca^{2+} to equilibrate for 15 min before initiating the reaction with 10μM PS/PC (30/70, w/w) vesicles. This procedure reduced the noise in the assay. The results (Figure 3-3) fit by non-linear least squares (Bevington, 1969) indicate that 0.5 nM VIIa was 50% saturated with 1.1 nM sTF. This experiment indicates that the K_d for the sTF:VIIa complex is 1 nM.

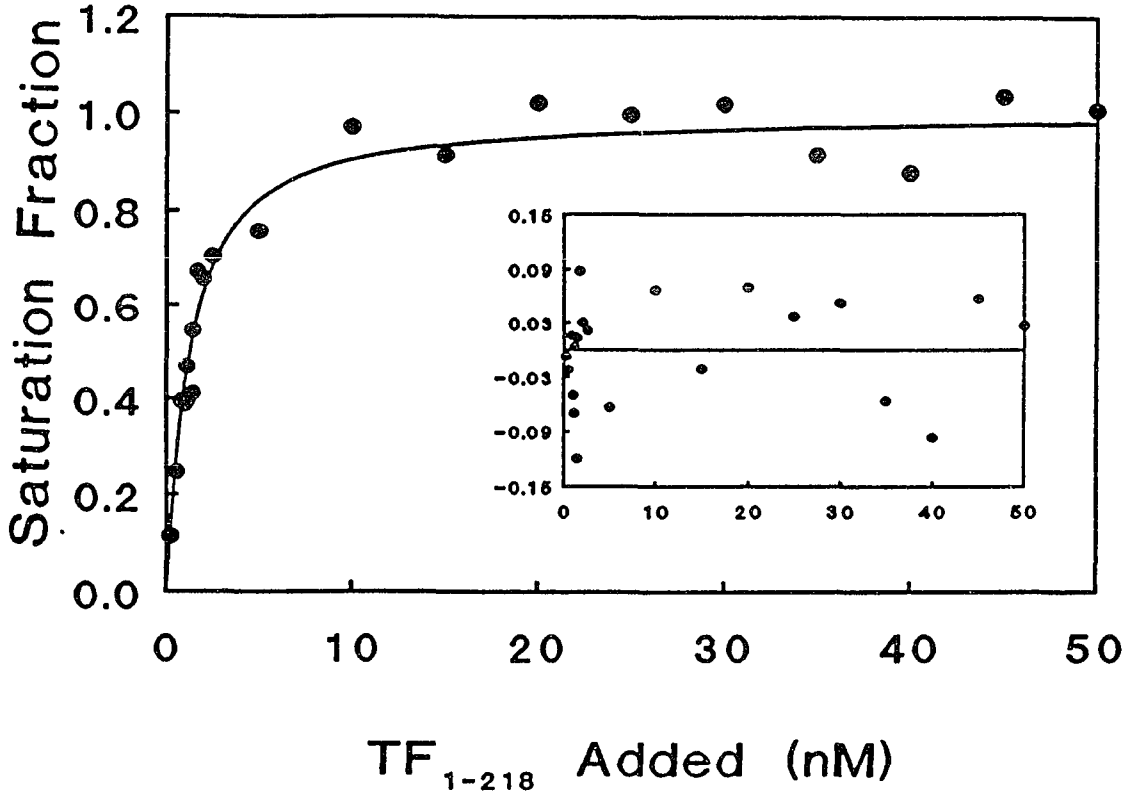

Figure 3-3. *Titration of VIIa with sTF:* VIIa (0.5 nM) was incubated for 15 min at 25° C with the indicated concentrations of sTF, factor X (250 nM), Ca^{2+} (5 mM) in 10 mM HEPES, 0.14M NaCl, 0.1% bovine serum albumin (BSA), pH 7.5. The reaction was initiated by the addition of 10 μM PS/PC (30/70, w/w). Aliquots (25 μL) were withdrawn every 0.5 min and added to 125 μL of 50 mM EDTA, 0.05% BSA, pH 7.5. A chromogenic substrate (Spectrozyme Xa, American Diagnostic, Greenwich, CT) was added (0.5 mM, final concentration). The rate of generation of the free chromophore was monitored at 405 nm.

DISCUSSION

Coagulation reactions are known to proceed much more rapidly on membrane surfaces than free in solution (see Mann et al., 1990, for a review). The mechanism of this acceleration has not yet been fully elucidated. In this regard, we and others have found that sTF, a soluble TF construct lacking the transmembrane domain, is much less active than TF_{1-263} , the full-length membrane-spanning form. In the present study, we have compared the binding of human VIIa to sTF and to TF_{1-263} reconstituted in PC vesicles to determine whether this reduced activity can be attributed to impaired binding of VIIa to sTF. This comparison required the development of a true equilibrium technique to measure the TF:VIIa association.

Previous studies by other groups have determined dissociation constants ranging from 82 pM to 9 nM for the interaction of VIIa with TF present on a variety of human cell lines (Broze, 1982; Rodgers et al., 1984; Ploplis et al., 1987; Fair & MacDonald, 1987). Each of these studies depended on the separation of bound VIIa from free VIIa. Accordingly, none were true equilibrium measurements. Similarly, in a study of the binding of bovine VII and VIIa to bovine TF in our laboratory (Bach et al., 1986), we obtained K_d values in the nanomolar range. That study also employed a non-equilibrium technique. A study by Warn-Cramer and Bajaj (1986), using a human brain TF extract and a purely kinetic approach, yielded a K_d ranging from 110 to 460 pM. More recently, a study by Ruf et al. (1991b) measured the binding of VIIa to detergent solubilized TF_{1-263} and to their own recombinant soluble TF using a technique in which TF was immobilized on a microtiter plate by a monoclonal antibody, previously shown to inhibit VIIa binding

by 20% (Morrissey et al., 1988). This group determined dissociation constants of 4.2 nM and 90.3 nM for detergent solubilized TF_{1-263} and the soluble TF construct, respectively. The wide range of values reported by these various studies points to the need for a study of the VIIa:TF interaction using both a well-defined TF preparation and an equilibrium binding technique capable of measuring tight associations.

We examined the interaction of sTF with VIIa using three independent approaches: 1) sedimentation equilibrium, 2) pressure-dependent fluorescence anisotropy, and 3) enzymatic titration. Pressure-dependent fluorescence anisotropy is a well-established technique for studying tight protein-protein interactions under equilibrium conditions. The three techniques yielded consistent results for sTF: a K_d of 0.6 to 1 nM. In addition, we examined the interaction of VIIa with full-length TF reconstituted in pure PC vesicles. The tighter association of VIIa with the full-length reconstituted TF precluded quantitation of the K_d for this interaction by any means other than pressure-dependent fluorescence anisotropy. The K_d obtained by this method was 7.3 pM, indicating a 2.6 kcal mol^{-1} difference in ΔG of these interactions.

Under the conditions we used to measure the activity of sTF, it is clear that at least 90% of sTF is complexed with VIIa. Consequently, the observed difference in its activity compared to TF_{1-263} cannot be the result of decreased complex formation. The dissociation constants determined in this study are markedly different from the values of 90.3 and 4.2 nM reported for sTF and TF_{1-263}, respectively, in a study by Ruf et al. (1991b). If these higher values were correct, the titration experiment (Figure 3-3) would have shown increasing sTF:VIIa activity over all concentrations used. Instead, our data

showed no increase in activity past 10 nM sTF, indicating that saturation of VIIa was achieved. We attribute these differences to differences in TF preparations and in methodology.

The 25-fold difference in activities of the sTF:VIIa and TF:VIIa complexes might conceivably be accounted for by an ordered addition of X to sTF:VIIa according to a model similar to that proposed for bovine TF:VIIa (Nemerson & Gentry, 1986). The pressure-dissociation and sedimentation equilbrium studies, however, did **not** contain X or lipid. Therefore, these experiments could not be affected by an ordered addition reaction mechanism. Furthermore, it is unlikely that the difference in the measured dissociation constants results from an affinity of the DF-VIIa for the lipid as there is no evidence that VIIa binds to pure PC vesicles (Bach et al., 1986). The 2.6 kcal mol^{-1} difference in ΔG and the two-fold difference in ΔV clearly indicate that the two complexes are structurally different. This lipid dependent structural change may be common to clotting enzymes. For example, the k_{cat} for the activation of prothrombin by Factor Xa increases by an order of magnitude upon addition of acidic phospholipids (Rosing, et al., 1980).

In accord with Ruf, et al., (1991a), we found that sTF:VIIa complex does not generate Xa in the absence of acidic phospholipids. Interestingly, TF_{1-263} is functional in PC vesicles whereas no activity was detected with sTF in the presence of PC alone (data not shown). The mechanism by which acidic vesicles function in the sTF-dependent reaction is unknown. While it is possible that these vesicles complex with substrate to form the true substrate for sTF:VIIa, as suggested by Ruf et al. (1991a), it is also possible

that sTF:VIIa forms a nonproductive ternary complex with X in the absence of lipids. In this model, interaction of the acidic phospholipid with the *ternary complex* is required for substrate turnover.

ACKNOWLEDGMENTS

We thank Drs. Catherine Royer and William Mantulin for help in preliminary high-pressure dissociation studies carried out at the laboratory for Fluorescence Dynamics at the University of Illinois, Urbana, Illinois, and we thank Dr. David Jameson for the loan of his high pressure sample chamber which was used in preliminary experiments. In addition, we thank Paul Contino for his invaluable assistance with the graphics and with preliminary experiments on the lipid dependence of sTF.

References for Chapter 3

Azumi, T. & McGlynn, S. P. (1962) *J. Chem. Phys. 37*, 2413-2420.

Bach, R., Nemerson, Y., & Konigsberg, W. (1981) *J. Biol. Chem. 256*, 8324-8331.

Bach, R. (1988) Initiation of coagulation by Tissue Factor *CRC Crit. Rev. Biochem. 23*, 339-368.

Bach, R., Gentry, R., & Nemerson, Y. (1986) *Biochemistry 25*, 4007-4020.

Bach, R., Konigsberg, W. H., & Nemerson, Y. (1988) *Biochemistry 27*, 4227-4231.

Bevington, P. R. (1969) *Data Reduction and Error Analysis for the Physical Sciences*, pp. 204-246, McGraw-Hill, New York, NY.

Broze, G. J., & Majerus, P. W. (1980) *J. Biol. Chem. 255*, 1242-1247.

Broze, G. J., (1982) *J. Clin. Invest. 70*, 526-535.

Di Scipio, R. G., Hermodson, M. A., Yates, S. G., & Davie, E. W. (1977) *Biochemistry 16*, 698-705.

Edgington, T. S., Mackman, N., Brand, K., & Ruf, W. (1991) *Thromb. and Haem. 66*, 67-79.

Fair, D. S., & MacDonald, M. J. (1987) *J. Biol. Chem. 262*, 11692-11698.

Heremans, K. (1982) *Ann. Rev. Biophys. Bioeng. 11*, 1-21.

Johnson, M. L., Correia, J. C., Yphantis, D. A., & Halvorson, H. R. (1981) *Biophys. J. 36*, 575-588.

Laue, T. M. (1981) *"Rapid Precision Interferometry for the Analytical Ultracentrifuge"*, Ph.D. dissertation, University of Connecticut, Storrs, CT.

Laue, T. M., Johnson, A. E., Esmon, C. T., & Yphantis, D. A. (1984) *Biochemistry 23*, 1339-1348.

Laue, T. M. (1992) *"Analytical Ultracentrifugation in Biochemistry and Polymer Science"*, Eds. S. Harding & A. Rowe, Royal Society of Chemistry, London.

Luckow, E. A., Lyons, D. A., Ridgeway, T. M., Esmon, C. T., & Laue, T. M. (1989) *Biochemistry 28*, 2348-2354.

Mann, K. G. , Nesheim, M. E., Church, W. R., Haley, P., & Krishnaswamy, S. (1990) *Blood 76*, 1-16.

Messing, J., (1983) *Methods Enzymol. 101*, 20-78.

Miletich, J. P., Broze, G. J., & Majerus, P. W. (1981) *Methods Enzymol. 80*, 221-228.

Mimms, L. T., Zampighi, G., Nozaki, Y., Tanford, C., & Reynolds, J. A. (1981) *Biochemistry 20*, 833-840.

Morrissey, J. H., Fair, D. S., & Edgington, T. S. (1988) *Thrombosis Research 52*, 247-261.

Olsen, P. H., Esmon, N. L., Esmon, C. T., & Laue, T. M. (1991) *Biochemistry, in press.*

Ploplis, V. A., Edgington, T. S., & Fair, D. S. (1987) *J. Biol. Chem. 262*, 9503-9508.

Nemerson, Y., & Gentry, R. (1986) *Biochemistry 25*, 4020-4033.

Paladini, A. A., & Weber, G. (1981) *Rev. Sci. Inst. 52*, 419-427.

Paoletti, J., & LePecq, J. B. (1969) *Anal. Biochem. 31*, 33-41.

Rodgers., G. M., Broze, G. J., & Shuman, M. A. (1984) *Blood 63*, 434-438.

Rosing, J., Tans, G., Govers-Riemslag, W. P., Zwaal, R. F. A., & Hemker, H. C. (1979) *J. Biol. Chem. 255*, 274-283.

Ruf, W., Rehemtulla, A., & Edgington, T. S. (1991a) *J. Biol. Chem. 266*, 2158-2166.

Ruf, W., Kalnik, M. W., Lund-Hansen, T., & Edgington, T. S. (1991b) *J. Biol. Chem. 266*, 15719-15725.

Silverberg, S. A., Nemerson, Y., & Zur, M. (1977) *J. Biol. Chem. 252*, 8481-8488.

Spicer, E. K., Horton, R., Bloem, L., Bach, R., Williams, K. R., Guha, A., Kraus, J., Lin, T. C., Nemerson, Y., & Konigsberg, W. H. (1987) *Proc. Natl. Acad. Sci. U.S.A. 84*, 5148-5152.

Thim, L., Bjoern, S., Christensen, M., Nicolaisen, E. M., Lund-Hansen, T., Pedersen, A. H., & Hedner, U. (1988) *Biochemistry 27,* 7785-7793.

Warn-Cramer, B. J., & Bajaj, S. P. (1986) *Biochem. J. 239,* 757-762.

Waxman, E., Ross, J.B.A., Laue, T.M., Guha, A., Thiruvikraman, S.V., Lin, T.C., Konigsberg, W.H., & Nemerson, Y. (1992) Biochemistry 31, 3998-4003.

Weber, G., & Drickamer, H. G. (1983) *Quart. Rev. Biophys. 16,* 89-112.

Wetlaufer, D. B. (1962) *Adv. Prot. Chem. 17,* 303-390.

Yanis-Perron, C., Biera, J., & Messing, J. (1985) *Gene 33,* 103-119.

Yphantis, D. A. (1960) *Ann. N.Y. Acad Sci. 88,* 586-601.

Yphantis, D. A. (1964) *Biochemistry 3,* 297-317.

CHAPTER 4

HUMAN FACTOR VIIa AND ITS COMPLEX WITH SOLUBLE TISSUE FACTOR: EVALUATION OF ASYMMETRY AND CONFORMATIONAL DYNAMICS BY ULTRACENTRIFUGATION AND FLUORESCENCE ANISOTROPY DECAY METHODS

from Waxman et al.1993

INTRODUCTION

The complexation of factor VIIa (VIIa)[1] with membrane-bound tissue factor (TF) is a critical step in the initiation of blood coagulation. TF is a transmembrane glycoprotein consisting of an extracellular domain (residues 1-219), a single transmembrane domain (residues 220-242), and a cytoplasmic domain (residues 243-263) which contains a half-cysteine residue thioesterified to palmitate or stearate (for review see Bach, 1988). When complexed with TF, the serine protease activity of VIIa towards its natural substrate, factor X (X), is increased by many orders of magnitude (Silverberg et al., 1977).

In vivo, complexation of TF and VIIa takes place at the vascular wall (for review see Nemerson & Turitto, 1991). Near the wall, viscous drag is exerted by the stationary vascular surface radially and by the bulk of the flowing blood medially. In this way high shear forces are generated. An asymmetric molecule *in solution near the wall* should thus tend to align parallel to the direction of flow. If the molecule is *anchored at the vascular wall* it should experience forces that may be important for determining conformation. This suggests two mechanisms by which a flowing environment could affect the kinetics of blood coagulation and other reactions that take place at the vascular surface.

In this paper, we present results from sedimentation and fluorescence anisotropy measurements that clearly demonstrate that VIIa and the complex it forms with sTF, a soluble truncation mutant of TF, are both highly asymmetric. In addition, we have

established that the binding of sTF to VIIa induces a conformational change in VIIa that leads to a loss in the segmental flexibility of VIIa in the domain containing the active site. In doing so, we have combined measurement of translational and rotational hydrodynamic properties in a useful way that may serve as a template for studies of other protein systems where asymmetry and flexibility would be of interest.

EXPERIMENTAL PROCEDURES

Experimental Approach. In the absence of X-ray crystal structure models for TF, VIIa, or the complex they form (TF:VIIa), there is a need to use other physical methods to assess their three-dimensional structures. The classical method for examining the global structure of a protein in solution is by assessment of its hydrodynamic properties using ultracentrifugation. Sedimentation equilibrium and sedimentation velocity experiments provide the molecular weight and the translational frictional coefficient of the macromolecule. The translational frictional coefficient, however, is a single parameter which depends on the size, shape, and flexibility of the molecule. Thus, it is impossible to distinguish between oblate (discus shaped) and prolate (cigar shaped) models using sedimentation velocity alone. Likewise, it is impossible to distinguish a flexible asymmetric molecule from a rigid molecule of lower asymmetry.

In this paper we demonstrate that time-resolved fluorescence anisotropy decay measurements provide additional information that can reduce the centrifuge determined range of possible shapes that are consistent with the hydronamic behavior of VIIa and the sTF:VIIa complex.

Figure 4-1 outlines the flow of information -- data, calculations, and assumptions-- that we used to place limits on the semiaxes of the general ellipsoid (Figure 4-2) that best represents the hydrodynamic behavior of VIIa and sTF:VIIa. Our initial observation is that the steady-state anisotropy of an active-site, dansyl-labelled VIIa prepared for

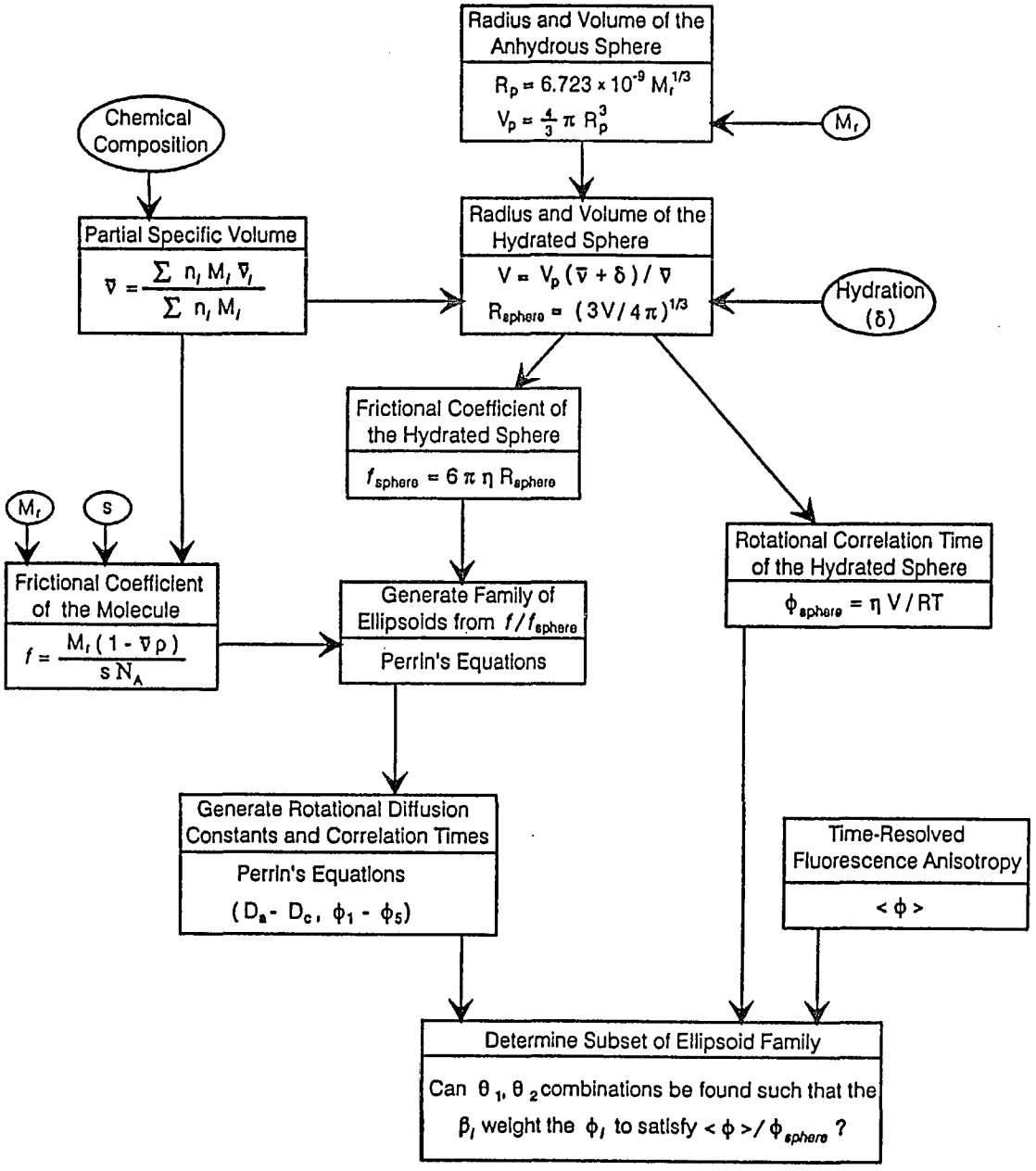

Figure 4-1. Flow diagram for evaluation of hydrodynamic parameters showing inputs, assumptions, procedures, and equations where appropriate. Steps are explained fully in Experimental Procedures.

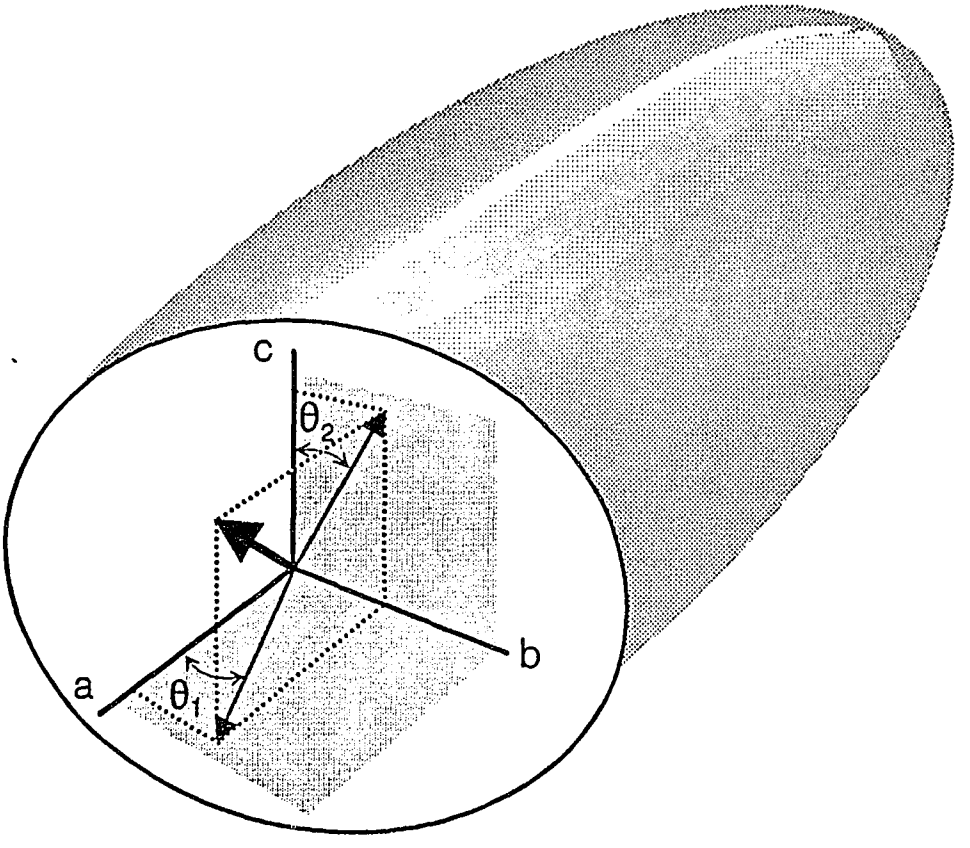

Figure 4-2. Representation of a general ellipsoid. The semiaxes of the ellipsoid are a, b, and c with $a \geq b \geq c$. We assume that the absorbance and emission transition dipole moments of the fluorophore, represented by the bold arrow, are coincident. θ_1 and θ_2 are the angles defining the orientation of the dipole moments with respect to the molecular axes. θ_1 is the angle to the major semiaxis a, and θ_2 is defined by the projection onto the plane of the b and c semiaxes.

thermodynamic studies (Waxman et al., 1992) indicates that neither VIIa nor sTF:VIIa is well represented by a monomeric sphere. To address whether the steady-state anisotropy reflects higher order associations of these molecules, we performed equilibrium ultracentrifugation experiments. Sedimentation velocity experiments were then performed to evaluate the deviation of the molecules from rigid spheres. Using equations derived by Perrin (1934), we generated a family of ellipsoids that are consistent with the centrifuge data for VIIa and sTF:VIIa. As discussed below, time-resolved fluorescence anisotropy experiments were then used to place additional limits on the family of ellipsoids and to distinguish between changes in the translational frictional coefficient due to asymmetry or those due to increased rigidity. This approach has been previously suggested by Small and Isenberg (1977) and Stafford and Szent-Györgyi (1978).

Calculation of R_{sphere}, the Radius of the Hydrated Stoke's Sphere. A useful and commonly applied first step in the evaluation of hydrodynamic observables is the calculation of values expected if the molecule were a rigid sphere. In this way, considerations of molecular size are factored out and only shape parameters -- asymmetry and flexibility -- need be considered. The first step shown in Figure 4-1 is the calculation of R_p, the radius of an anhydrous sphere with a molecular weight equal to that of the molecule of interest. For this we used the empirical equation

$$R_p = 6.723 \times 10^{-9} M_r^{1/3} \qquad (1)$$

where M_r is the molecular weight obtained from equilibrium centrifugation (Teller, 1976).

This relationship is based on packing volumes observed in X-ray crystallographic structures of protein-protein complexes. The anhydrous molecular volume, V_p, can be calculated from R_p. It has been shown that the classical textbook formulation,

$$R_o = \sqrt[3]{\frac{3M_r\bar{\nu}}{4\pi N_A}}, \qquad (2)$$

where N_A is Avogadro's number and $\bar{\nu}$ is the partial specific volume of the protein, underestimates the radii and leads to overestimates of the axial ratios in subsequent calculations (Laue et al., 1992).

The hydration, δ, is used in the next step to generate V, the volume of the *hydrated* sphere.

$$V = V_p\left(\frac{\bar{\nu}+\delta}{\bar{\nu}}\right). \qquad (3)$$

$\bar{\nu}$ is estimated using the method of Cohn and Edsall (1943; Laue et al., 1992)

$$\bar{\nu} = \frac{\Sigma n_i M_i \bar{\nu}_i}{\Sigma n_i M_i} \qquad (4)$$

where n_i, M_i, and $\bar{\nu}_i$ are the number of moles, molecular weight, and partial specific volumes, respectively, for the components -- amino acids and carbohydrates -- which make up the protein. For the purposes of this development, δ was estimated at 0.280 g H_2O/g protein. This value is an average of data from sedimentation velocity and small-angle X-ray scattering experiments for a group of proteins with molecular weights less than 100,000 (Pessen and Kumosinski, 1985). R_{sphere}, the radius of the *hydrated* Stokes

sphere, is easily calculated from V.

Sedimentation Velocity; Calculation of f_{sphere}. For a rigid, spherical particle, Stokes' law predicts that the translational frictional coefficient is given by

$$f_{sphere} = 6\pi\eta R_{sphere} \tag{5}$$

where η is the solvent viscosity.

Evaluation of f and Calculation of the Friction Ratio. The rate, v, at which a molecule sediments in a centrifugal field $\omega^2 r$ is given by the Svedberg equation

$$s = \frac{v}{\omega^2 r} = \frac{M_r(1-\bar{v}\rho)}{N_A f} \tag{6}$$

where s is the sedimentation coefficient for the molecule, f is the frictional coefficient, ρ is the solvent density, ω is the angular velocity, and r is the distance of the molecule from the center of the field.

An asymmetric particle will have a frictional coefficient greater than that of a spherical particle of the same volume. Thus the friction ratio, f/f_{sphere}, is often used to calculate the axial ratios for prolate and oblate ellipsoids which are consistent with the behavior of the molecule in the centrifuge. There is no reason, however, to believe that a protein is well represented by either an oblate or prolate ellipsoid and, in fact, for a given friction ratio the oblate and prolate models provide the most extreme cases of

deviation from a sphere. If we take the semiaxes of an ellipsoidal structure to be a, b, and c with a > b > c (Figure 4-2), then for a rigid particle the friction ratio defines a family of rigid ellipsoids ranging in flatness (b/c) and elongation (a/b) from the oblate case to the prolate. The family of ellipsoids consistent with a given friction ratio can be generated by numerical evaluation of Perrin's equation (Perrin, 1934) as outlined by Small and Isenberg (1977). Initially, semiaxis a is set equal to semiaxis b. Semiaxis c is numerically evaluated to obtain the axial ratio for the oblate case. Semiaxis c is then numerically evaluated for increasing values of a/b until the prolate case, b=c, is reached. The result of this procedure is a table of b/c versus a/b for ellipsoids with the experimentally-determined friction ratio.

If an asymmetric molecule is not rigid, any segmental flexibility will lower the friction ratio compared to that of the fully extended molecule. Sedimentation velocity experiments measure the time-averaged shape of the molecule. Thus, the friction ratio defines a family of ellipsoids that represent the time-averaged shape of the molecule and it is impossible, using sedimentation methods alone, to distinguish between a highly asymmetric flexible molecule and a rigid molecule of lower asymmetry.

Fluorescence Anisotropy; Calculation of ϕ_{sphere} . For fluorophores bound to a macromolecule, the rate at which the chromophore rotates, and therefore the polarization of its emitted light, will be affected by the size, shape, and flexibility of the macromolecule as well as by the orientation of the fluorophore to the macromolecular

axes. For a fluorophore rigidly attached to a rigid spherical molecule, the rotational correlation time, ϕ_{sphere}, may be calculated from the Stokes-Einstein equation

$$\phi_{sphere} = \frac{\eta V}{RT} \quad . \tag{7}$$

In this equation, R is the gas constant, η is the solution viscosity, and T is the temperature.

Evaluation of $<\phi>$ and the Rotational Ratio. Two types of experiments are typically performed to assess the rotational correlation time, ϕ, of a fluorophore. In a steady-state fluorescence anisotropy experiment, the solution is excited continuously and fluorescence is detected through vertically and horizontally oriented polarizers. The amount of depolarization is expressed as the steady-state anisotropy, <r>,

$$<r> = \frac{I_v - I_h}{I_v + 2I_h} \tag{8}$$

where I_v and I_h are the intensities detected through vertical and horizontal polarizers when vertical light is used to excite the sample. The measured steady-state anisotropy will be

$$<r>_{sphere} = \frac{<r>_o}{1 + \tau/\phi_{sphere}} \tag{9}$$

where $<r>_o$ is the zero-point or 'frozen' anisotropy extrapolated back to infinite solvent viscosity, and τ is the intensity lifetime of the fluorophore. The degree to which a

macromolecule deviates from a rigid sphere may be assessed by comparing the measured <r> to $<r>_{sphere}$. Asymmetry will cause the measured <r> to shift toward $<r>_0$ and to exceed $<r>_{sphere}$. If the macromolecule is not rigid or the fluorophore has depolarizing motions independent of the macromolecule, these segmental motions will cause the measured <r> to shift toward 0 and to be less than $<r>_{sphere}$. In addition, the orientation of the probe with respect to the macromolecular axes is important in determining the degree to which asymmetry and flexibility cause deviation from $<r>_{sphere}$ (see below).

In a time-resolved fluorescence anisotropy experiment the sample is repetitively pulsed with polarized light. By analogy with Equation 8, the time dependence of the depolarization due to rotation is measured as

$$r(t) = \frac{I_v(t) - I_h(t)}{I_v(t) + 2I_h(t)} . \qquad (10)$$

For a fluorophore rigidly attached to a rigid spherical molecule, the anisotropy decay law is given by

$$r(t) = r_o e^{-t/\phi_{sphere}} \qquad (11)$$

where r_0 is the anisotropy extrapolated back to time zero. For a fluorophore rigidly attached to a non-spherical molecule, the anisotropy decay is considerably more complicated. It has been shown that the the anisotropy decay law for an ellipsoidal molecule is a sum of five exponentials (Tao, 1969; Belford et al., 1972). Calculation of the relative values of the correlation times of these exponentials for ellipsoids of varying

$$r(t) = \sum_{i=1}^{5} \beta_i e^{-t/\phi_i} \quad . \tag{12}$$

axial ratios show that only three values of ϕ_i are sufficiently distinct to be resolvable even under ideal circumstances (Small & Isenberg, 1977). In protein studies, however, often only a single exponential decay with a ϕ equal to the mean correlation time

$$\langle\phi\rangle = \left[\frac{\sum \beta_i/\phi_i}{\sum \beta_i}\right]^{-1} \tag{13}$$

is observed. The preexponential weighting factors, β_i, and therefore $\langle\phi\rangle$, are complicated functions of both the asymmetry of the protein and the orientation of the fluorophore's absorbance and emission dipoles with respect to the axes of the protein. For example, for a fluorophore that has coincident absorbance and emission dipoles and is attached to a prolate ellipsoid shaped protein, $\langle\phi\rangle$ will be maximal if the dipoles are aligned parallel to the long axis ($\theta_1 = 0$ in Figure 4-2) and minimal when the dipoles are aligned parallel to the short axis ($\theta_1 = 90°$ in Figure 4-2).

Because $\langle\phi\rangle$ depends on orientation of the probe as well as the size, shape, and flexibility of the molecule, the rotation ratio, $\langle\phi\rangle/\phi_{sphere}$, places fewer constraints on the range of ellipsoids that can represent the behavior of the molecule than the friction ratio does. However, because the rotation ratio depends on asymmetry differently than the friction ratio does, the rotation ratio can be used to place further limits on the family of

ellipsoids generated using the friction ratio. First, $<\phi>$ is measured and the rotation ratio is calculated. Then, Perrin's equations are used to calculate the three rotational diffusion coefficients (D_a, D_b, D_c) and five correlation times for each of the members of the friction ratio-consistent table of ellipsoids. Finally, the range of ellipsoids consistent with both the friction and rotation ratios is determined. This is accomplished by evaluating, for each ellipsoid, whether a probe orientation can be found such that the β_i's (Equation 13) weight the five exponentials so that the experimentally-determined rotation ratio is recovered. The equations for determining the β_i's for different probe angles are outlined by Belford et al. (1972).

In addition to limiting the range of ellipsoids which can represent the hydrodynamic behavior of a molecule, time-resolved fluorescence anisotropy decay data can provide important information regarding molecular flexibility or segmental motion which cannot be inferred from the sedimentation data. This is due to the short time frame (ps to ns) over which rotation is measured. In time-resolved fluorescence anisotropy measurements, segmental motion of a region of the protein containing the probe will produce a component in the anisotropy decay with a correlation time less than ϕ_{sphere}. The appropriate equation for the anisotropy decay in this case is

$$r(t) = r_o[\gamma e^{-t/\phi_{segmental}} + (1-\gamma)]e^{-t/\phi_{global}} \qquad (14)$$

where γ is a scaling factor between 0 and 1 (see Lakowicz, 1983). In this equation, $\phi_{segmental}$ is the correlation time for depolarizing motions of a domain containing the probe

and ϕ_{global} is the correlation time for the rotational motion of the protein as a whole. Anisotropy decay data is typically analyzed as a sum rather than a product of exponentials, so that the decay law in the presence of segmental flexibility is observed to be

$$r(t) = r_o[\, p_{short} e^{-t/\phi_{short}} + p_{long} e^{-t/\phi_{long}}] \qquad (15)$$

where $p_{short} = \gamma$ and $p_{long} = 1 - \gamma$. Thus,

$$\phi_{short}^{-1} = \phi_{segmental}^{-1} + \phi_{global}^{-1} ; \quad \phi_{long}^{-1} = \phi_{global}^{-1} . \qquad (16)$$

An anisotropy decay which analyzes as a biexponential with one correlation time greater than or equal to ϕ_{sphere} and one less than ϕ_{sphere} can thus be diagnostic for segmental motion of a domain of the macromolecule containing the probe.

Proteins: Human recombinant VIIa was a generous gift of Dr. Ulla Hedner, Novo Nordisk, Copenhagen. Fluorescence anisotropy studies were performed using dansyl-labelled VIIa (DF-VIIa) covalently modified at its active site histidine with dansyl-D-Phe-L-Phe-Arg-chloromethyl ketone as described previously (Waxman et al., 1992). Briefly, DFVIIa was separated from free dansyl-FFRCk on a Sephadex G-15 column. Protein and dansyl concentrations were measured by absorbance and the labeling ratio observed was

1 mol dansyl to 1 mol of VIIa when VIIa was fully inhibited[1]. SDS-PAGE run under reducing conditions showed that the fluorescent label was bound exclusively to the heavy chain of VIIa as would be expected for this active site specific modification.

Studies of the TF:VIIa complex are complicated by the requirement that full-length TF be reconstituted in phospholipid vesicles or solubilized in detergent. This makes the possible interactions of TF and VIIa which involve the lipid or detergent difficult to resolve from those due strictly to direct protein-protein interactions, and complicates the thermodynamic description of the TF:VIIa interaction. Furthermore, a hydrodynamic study of the complex would be difficult to interpret since global motions of the complex would be dominated by the overall motion of the lipid vesicles. In the present studies, we make use of a soluble TF (TF_{1-218}; sTF) which lacks the transmembrane and cytoplasmic domains. This material was prepared and purified as described previously (Waxman et al., 1992).

Ultracentrifugation Experiments: Sedimentation equilibrium studies of the sTF:VIIa complex were performed at 23.3° C in a Beckman Model E analytical ultracentrifuge equipped with an electronic speed control, RTIC temperature controller,

---

[1]The extinction of human VIIa at 280 nm was based on the number of tryptophan and trysosine residues in recombinant VIIa (Thim et al., 1988) using average extinction coefficients for tryptophan (5,500 $M^{-1}cm^{-1}$) and tyrosine (1,200 $M^{-1}cm^{-1}$) residues in a protein (Wetlaufer, 1962). The extinction of DF-VIIa was calculated using the extinction coefficients for ϵ-dansyl-lysine in water (J.B.A. Ross, unpublished data) and our calculated value for the extinction of VIIa at 280 nm, assuming additivity of the absorptions.

Rayleigh interference optics, and a pulsed laser diode light source (670 nm). Data was acquired using a television-camera-based, on-line data acquisition and analysis system (Laue, 1981; Laue et al., 1992). Samples were loaded into short column cells (0.7 mm) (Yphantis, 1960) at several concentrations up to 1 mg/mL total protein. Data were collected at intervals after the estimated equilibrium time and tested for equilibrium by subtracting successive scans (Yphantis, 1964). M_r was estimated using the nonlinear squares analysis program NONLIN (Johnson et al., 1981) as described previously (Laue et al., 1984).

Sedimentation velocity experiments were performed on a Beckman XLA analytical centrifuge equipped with absorption optics that allow scanning at multiple wavelengths and interfaced to a microcomputer for data acquisition. The sedimentation coefficient was determined from the movement of the boundry (Stafford, 1992) and corrected to standard conditions (20.0°C) and zero protein concentration using conventional methods (van Holde, 1985; Teller, 1973).

Fluorescence Experiments: Time-resolved fluorescence intensity and anisotropy measurements were obtained by the time-correlated single-photon counting method using an instrument previously described (Hasselbacher et al., 1991a). Decay curves were collected into either 2,000 or 4,000 channels, yielding a resolution of 22 or 11 ps per channel, respectively. Fluorescence decays were measured using excitation at 330 nm with detection through a 10 nm bandpass filter centered at 530 nm and a polarizer set

vertically, horizontally or at the magic angle (Badea & Brand, 1979). Fluorescence decay data were analyzed using nonlinear least squares regression (Bevington, 1969). The fluorescence intensity decay collected at the magic angle, $I_m(t)$, was fit to a sum of exponentials

$$I_m(t) = \sum_{i=1}^{n} \alpha_i e^{-t/\tau_i} , \qquad (17)$$

where τ_i is the lifetime and α_i is the amplitude of the *i*th component. The intensity-weighted mean lifetime, $<\tau>$, is defined by the relationship

$$<\tau> = \sum_{i=1}^{n} \alpha_i \tau_i^2 \; / \; \sum_{i=1}^{n} \alpha_i \tau_i \qquad (18)$$

The decay of the emission anisotropy was analyzed as a sum of exponentials (Eq. 12). The anisotropy parameters were obtained by fitting the vertically and horizonatally polarized emission decay curves ($I_v(t)$ and $I_h(t)$), using an approach similar to that described by Cross and Fleming (1984). To help constrain the intensity decay parameters (Equation 17) and provide a means for scaling the $I_v(t)$ and $I_h(t)$ curves to each other, we included the $I_m(t)$ curve in the analysis and fit all the data simultaneously according to the relationships:

$$\begin{aligned} I_v(t) &= \tfrac{1}{3}\, I_m(t) \times (1 + 2\sum \beta_j e^{-t/\phi_j}) \\ I_h(t) &= \tfrac{1}{3}\, I_m(t) \times (1 - \sum \beta_j e^{-t/\phi_j}) \; . \end{aligned} \qquad (19)$$

RESULTS

Intensity Decay Measurements: Intensity decay measurements were performed using 6 μM DFVIIa alone and in the presence of 10 μM sTF. Measurements were performed in 0.05 M Tris buffer, 0.1 M NaCl, and 5 mM $CaCl_2$, pH 7.5. No free DFVIIa is expected in the sample containing sTF as the dissociation constant (0.59 nM) is well below the concentrations used (Waxman et al., 1992). The intensity-weighted mean fluorescence lifetimes, $<\tau>$, ranged from 11.1 ns at 25°C to 12.4 ns at 5°C. No change in $<\tau>$ was seen upon addition of sTF. The relatively long $<\tau>$ compared to literature values for dansylated proteins (see Hasselbacher et al., 1991b) and the small dependence of $<\tau>$ on temperature both suggest that the dansyl group is shielded from solvent as would be expected if it were buried in the active site of VIIa. In addition, the emission spectrum of DFVIIa is blue-shifted approximately 12 nm relative to that of ϵ-dansyl-lysine. This is consistent with the suggestion that the dansyl group is buried in the active site.

Recognizing that the dansyl probe is specifically placed, we make the assumption that each of the lifetime components of the intensity decay is associated with the same molecular motions of the protein. In this case, the mean lifetime, $<\tau>$, conveys no less information than the individual decay components. Consequently, the $<\tau>$ of 11.1 ns at 25°C may be used to generate apparent rotational correlation times from steady-state anisotropy values for DFVIIa and sTF:DFVIIa obtained previously (Waxman et al., 1992). In that study, the steady-state anisotropy at 25°C was 0.234 for DFVIIa alone and 0.254

for DFVIIa in the presence of saturating amounts of sTF. This anisotropy change could be reversed by addition of EDTA. Using Equation 9 and an $\langle r \rangle_0$ of 0.32 for the dansyl probe (obtained from a Perrin plot of DFVIIa) yields apparent mean rotational correlation times of 30 and 43 ns for DFVIIa and sTF:DFVIIa, respectively. From Equation 7, the rotational correlation times of hydrated spheres (0.28 g water/g protein) with same molecular weights as these species would be 22 and 32 ns, respectively. These data suggest that the shapes of DFVIIa and the sTF:DFVIIa complex are not well represented by hydrated spheres. Considering the assumptions involved, it is impossible to determine from these data whether the large correlation times are due to asymmetry or higher order association. To resolve this question we turned to ultracentrifugation experiments.

Ultracentrifugation Studies: Table 4-1 shows the results obtained at each step of the procedure described in the Experimental Approach section and outlined in Figure 4-1. The M_r values obtained from equilibrium ultracentrifugation of VIIa, sTF, and an equimolar mixture of sTF and VIIa were 49,000, 27,700, and 73,700, respectively. These values are consistent with those obtained previously (Waxman et al., 1992). As before, neither sTF nor VIIa show a tendency towards reversible self-association at the concentrations employed. No dissociation of the sTF:VIIa complex was observed at these concentrations, consistent with the dissociation constant of 0.59 nM previously obtained (Waxman et al., 1992).

TABLE 4-1: Calculation of Hydrodynamic Parameters[a]

Parameter	VIIa	sTF:VIIa
M_r (g/mole)[b]	49000	73700
R_p (cm)	2.50e-07	2.80e-07
V_p (mL)	6.20e-20	9.40e-20
$\bar{v}$ (mL/g)	0.703	0.711
δ	0.28	0.28
V (mL)	8.70e-20	1.30e-19
R_{sphere} (cm)	2.80e-07	3.20e-07
f_{sphere} (g / sec)	5.20e-08	5.90e-08
$s^o_{20,w}$ (sec)[c]	3.4e-13	3.9e-13
f (g / sec)	7.20e-08	9.10e-08
f/f_{sphere}[d]	1.39	1.52
ϕ_{sphere} (ns)[e]	22	32
$\langle\phi\rangle$ (ns)[e]	94	123
$\langle\phi\rangle/\phi_{sphere}$	4.27	3.73

[a]Values have been rounded off for the purpose of presentation. [b]The estimated error in M_r is ± 2%. [c]The estimated error in s is ± 0.1e-13 sec. [d]Propagation of error indicates a ± 3% error in f/f_{sphere}. Intermediate values were not rounded for the actual calculations. [e]Correlation times presented are for 20 °C.

Sedimentation velocity experiments performed using VIIa and the equimolar mixture of sTF and VIIa both showed a single boundary. The translational frictional coefficients shown in Table 4-1 are calculated according to Equation 6. f_{sphere} for VIIa and sTF:VIIa are shown for comparison and the friction ratios f/f_{sphere} are calculated. As discussed above, each friction ratio is consistent with a family of ellipsoidal shapes ranging from prolate to oblate. For VIIa alone, the axial ratios for the oblate and prolate ellipsoids consistent with the determined friction ratio are 8.4 and 7.2 respectively. For sTF:VIIa, the axial ratios are 11.8 and 9.6 for the oblate and prolate ellipsoids.[2] Figure 4-3 shows b/c versus a/b for the family of ellipsoids consistent with the friction ratios obtained. In examining this figure, it is useful to note that the intercepts of the friction ratio-consistent curve at a/b = 1 and b/c = 1 represent the oblate and prolate ellipsoids respectively. Clearly, VIIa and sTF:VIIa are both highly asymmetric. Furthermore, the friction ratio for sTF:VIIa exceeds that of VIIa alone. However, as discussed above, the translational frictional coefficients alone are not sufficient to distinguish among the family of ellipsoids nor are they capable of distinguishing between a highly asymmetric flexible molecule and a rigid molecule with lower asymmetry. We therefore performed fluorescence anisotropy decay measurements to narrow further the range of ellipsoids

---

[2]One reviewer questioned how the choice of equation 1 rather than equation 2 for the calculation of the radius of an unhydrated spherical protein could alter our results. The use of equation 2 would yield unhydrated radii that are 2 - 4% smaller than those calculated using equation 1. Use of these smaller radii in subsequent calculations would yield axial ratios approximately 5 - 10% larger, and would suggest that VIIa and the sTF:VIIa complex are even more asymmetric. The general conclusions of the paper, however, are unaffected by personal preference regarding equations 1 or 2.

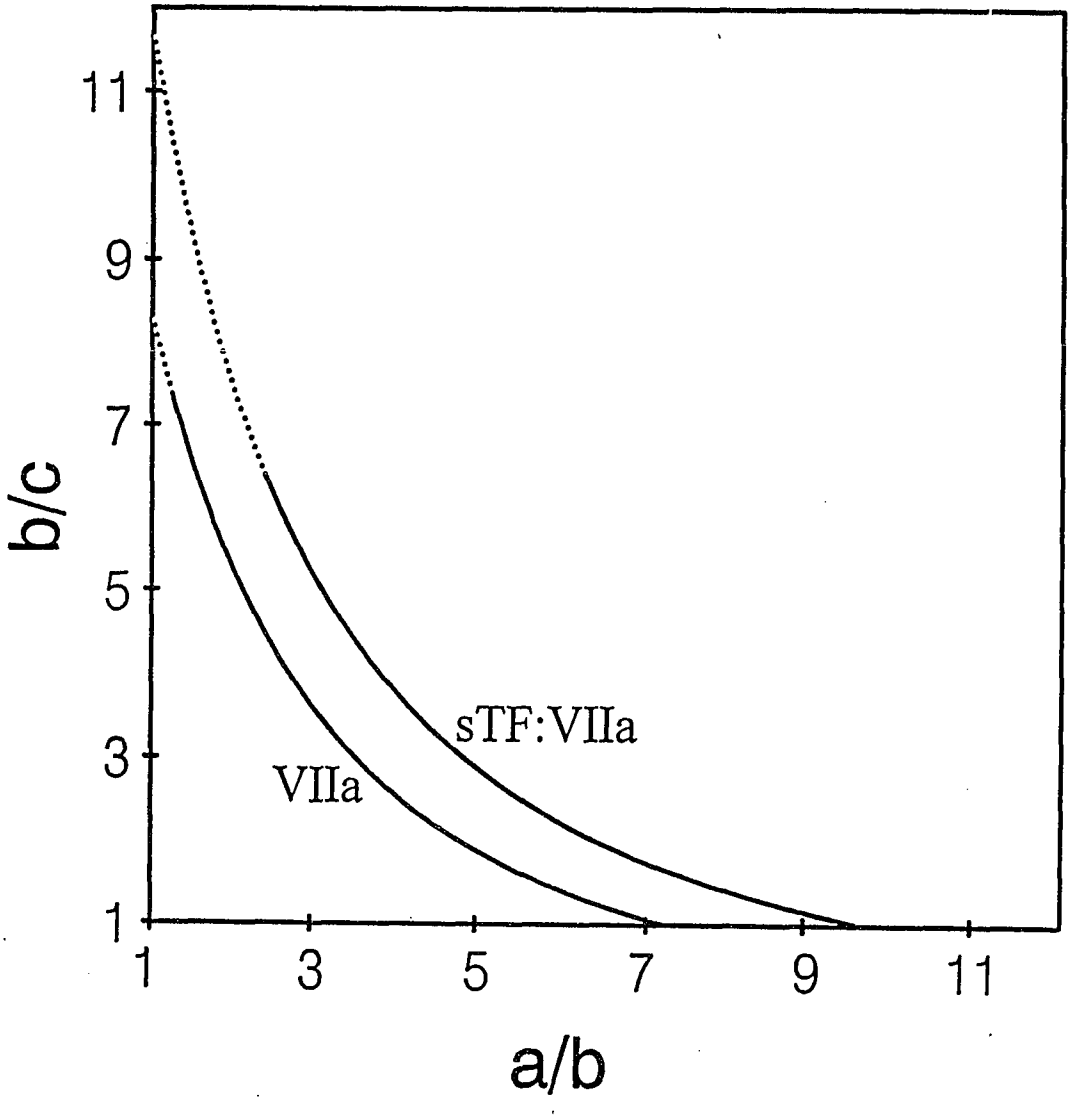

Figure 4-3. Flatness (b/c) versus elongation (a/b) for the family of ellipsoids consistent with the friction ratios determined for VIIa and sTF:VIIa. The solid part of the curves represent the subset of ellipsoids consistent with both the friction and rotation ratios.

which are consistent with the hydrodynamic behavior of VIIa and sTF:VIIa and to assess the extent to which segmental motions may be occurring.

Fluorescence Anisotropy Decay Studies: The results from the time-resolved fluorescence anisotropy experiments with DFVIIa and sTF:DFVIIa are shown in Table 4-2. Conditions were identical to those used for the intensity decay measurements. In all data sets where DFVIIa was observed alone, a biexponential model was necessary to fit the data. Although the pre-exponential of the shorter lived decay component was consistently only about 10% that of the longer lived decay component, the quality of the fit was clearly improved by the addition of this component. As noted above, the ϕ_{sphere} for VIIa at 20°C is 22 ns. When this value is compared to the correlation times obtained at this temperature it can be seen that the 97 ns correlation time is considerably larger than ϕ_{sphere}, and the 14 ns correlation time is considerably smaller than ϕ_{sphere}. This pattern suggests that the anisotropy decay of DFVIIa is composed of decays due to global and segmental motions. From Equations 14-16 it can be seen that the larger correlation time is equal to global motion correlation time, ϕ_{global}. A simple calculation (Equation 16) shows that the segmental motion correlation time is 12 ns. Equation 7 can be used to make an order of magnitude approximation of the size of the protein domain responsible for the fast component of the anisotropy decay. This analysis yields a molecular weight of approximately 30,000 and suggests that a significant fraction of the protein is involved. In addition, it is consistent with the other spectroscopic evidence that indicates that the dansyl probe is buried in the active site of VIIa.

Figure 4-4 shows the temperature and viscosity dependence of ϕ_{long} and ϕ_{short}. The correlation times used for this graph were obtained by fixing β_{long} and β_{short} to the average of their respective values obtained from initial analyses where all fitting parameters were iterated. The fitting statistics were unchanged by this procedure and the reproducibility of the correlation times was greatly improved. Also, the behavior of the correlation times as a function of η/T obeys the Stokes-Einstein equation (Equation 7) as would be expected if the correlation times reflected a global rotation and a large-scale segmental motion of DFVIIa. The observed dependence of the shorter correlation time on solution viscosity is particularly notable as it would not be expected if the faster component of the anisotropy decay were due to rapid motion of the probe within the active site of VIIa. The large value for ϕ_{long} as compared to ϕ_{sphere} is further evidence that DFVIIa is highly asymmetric.

In contrast to the data obtained for DFVIIa alone, the anisotropy decay of the sTF:DFVIIa complex was best modeled as a single exponential. There was no improvement in any of the fitting statistics criteria when a biexponential model was used for analysis. In fact, when the data for the complex were analyzed by a biexponential model, degenerate correlation times were were obtained. At 20°C, ϕ_{sphere} for sTF:DFVIIa is 32 ns. By contrast, the correlation time obtained from analysis of the anisotropy decay is 122 ns indicating, in agreement with the sedimentation data, that sTF:DFVIIa is also highly asymmetric. Figure 4-4 also shows the temperature and viscosity dependence of the correlation time of the sTF:DFVIIa complex. As observed for DFVIIa alone, the

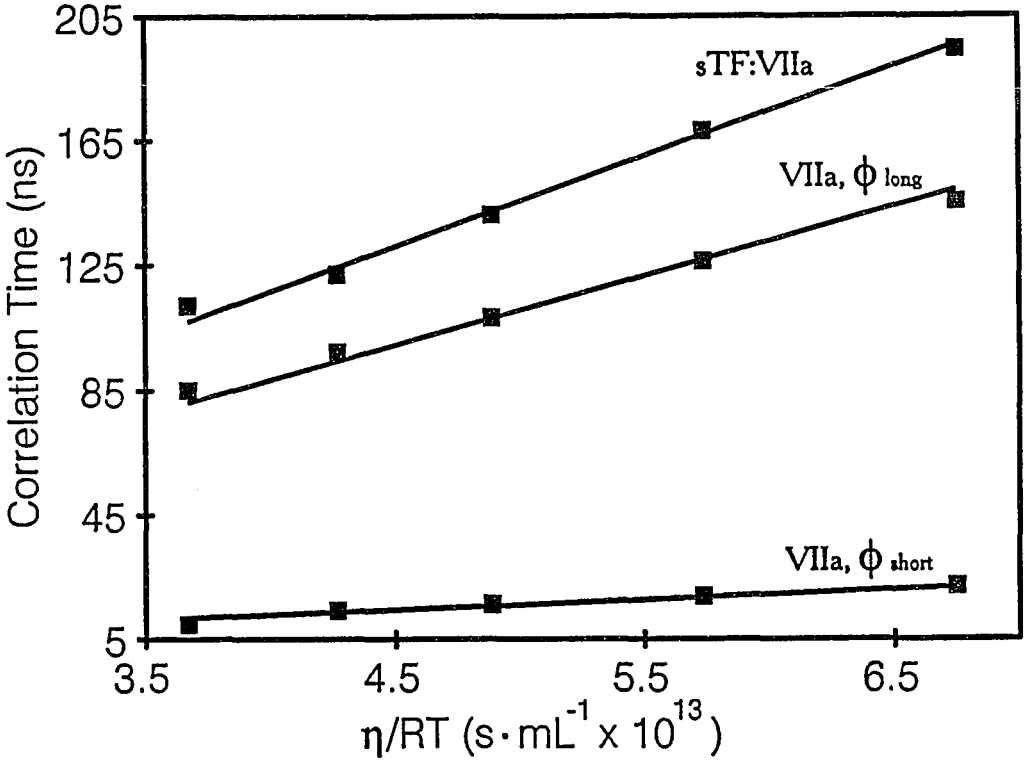

Figure 4-4. Correlation times versus η/RT for the DFVIIa and sTF:DFVIIa. A single exponential model fit the anisotropy decay of sTF:DFVIIa. Both the long and short correlation time for the biexponential model used for DFVIIa alone are shown. Details are described in Results.

TABLE 4-2: Time-Resolved Fluorescence Anisotropy Parameters[a]

Sample	T (°C)	η (cp)	β_1	ϕ_1 (ns)	β_2	ϕ_2 (ns)
DFVIIa	5	1.56	0.36	145	0.04	22.0
	10	1.35	0.36	126	0.04	18.6
	15	1.17	0.36	108	0.04	16.1
	20	1.04	0.36	97	0.04	14.1
	25	0.91	0.36	85	0.04	9.6
sTF:DFVIIa	5	1.56	0.40	194		
	10	1.35	0.39	168		
	15	1.17	0.40	141		
	20	1.04	0.40	122		
	25	0.91	0.40	112		

[a]The results presented for DFVIIa were obtained by fixing each β_i to the average value obtained from unrestricted analyses as described in Results. The results presented for sTF:DFVIIa are values obtained from completely unrestricted analyses.

dependence of the correlation time on η/T obeys the Stokes-Einstein equation (Equation 7).

In the final step of the analysis outlined in the Experimental Approach we used Perrin's equations as outlined by Small and Isenberg (1977) to generate the three principal rotational diffusion constants and five rotational correlation times for the family of ellipsoids consistent with the friction ratios obtained for VIIa and sTF:VIIa (Table 4-1). We then determined the subset of each family that was consistent with both the rotation and friction ratios (Figure 4-3). For VIIa alone, the ellipsoids consistent with both the friction and rotation ratios range from the prolate to an ellipsoid with axial ratios of a/b and b/c of 1.3 and 7.2, respectively. The corresponding molecular axes are 204×28×28 Å for the prolate ellipsoid and 126×98×14 Å for the other limiting shape. For sTF:VIIa the ellipsoids consistent with both the friction and rotation ratios range from the prolate to an ellipsoid with axial ratios of a/b and b/c of 2.37 and 6.41, respectively. The corresponding molecular axes are 254×26×26 Å for the prolate ellipsoid and 186×78×12 Å for the other limiting shape. Thus, for both VIIa and sTF:VIIa, a subset of flattened shapes is eliminated when the rotation ratio is taken into account. In particular, this analysis clearly demonstrates that an oblate model cannot account for the hydrodynamic behavior of either VIIa or its complex with sTF.

DISCUSSION

In vivo, complexation of TF and VIIa takes place at the vascular wall (Nemerson & Turitto, 1991). Shear stresses from blood flow in this region are high. Evidence from enzyme kinetic studies of TF:VIIa in a flowing reactor system suggests that the intrinsic activity of the complex is strongly affected by these shearing effects (Gemmell et al., 1990). Possible mechanisms for this effect include shear-induced conformational change or an increase in the probability of successful collisions due to preferred orientations of the enzyme and substrate under conditions of flow. Either mechanism, of course, would require that some or all of the molecules are asymmetric. With regard to this, several studies have provided evidence that suggest that other members of the clotting factor family are asymmetric (Lim et al., 1977; Laue et al., 1984; Isaacs et al., 1986; Husten et al., 1987; Luckow et al., 1989; Olsen et al., 1992). In this paper, we have investigated the hydrodynamic properties of VIIa and sTF:VIIa by sedimentation velocity and fluorescence anisotropy decay measurements. The combined data clearly demonstrate that VIIa and the complex it forms with sTF are highly asymmetric.

In addition, the anisotropy decay data show differences in the conformational dynamics of VIIa alone and bound to sTF. Specifically, a biexponential model is necessary to adequately describe the decay of the fluorescence anisotropy of VIIa. Multiexponential anisotropy decays have been observed for proteins which exhibit segmental flexibility. For example, Yguerabide et al. (1970) observed a biexponential decay with correlation times of 33 and 168 ns for dansyl-lysine bound to IgG. The longer correlation time, which exceeds ϕ_{sphere} for the 150,000 D protein, was attributed to the

global rotation of the protein while the shorter correlation time, which is less than ϕ_{sphere}, was attributed to segmental motions of the F_{ab} fragments. That result is essentially identical with what we have observed for VIIa in the absence of sTF. The shorter correlation time, 14 ns at 20°C, is significantly less than ϕ_{sphere} but substantially longer than expected for side chain motions (< 1 ns). It is likely that this short correlation time represents the jointed motion of a structural domain of VIIa that contains the labeled active site.

It could be argued that the improvement in the statistics obtained when the anisotropy decay of DFVIIa is fit to a biexponential decay law reflects the presence of three potentially resolvable anisotropy decay constants and not the presence of segmental motion. To test this possibility, we analyzed simulated data created with an intensity decay identical to that observed for DFVIIa and anisotropy decay parameters corresponding to those of several of the rigid ellipsoids consistent with the mean correlation time of VIIa. All correlation times recovered were greater than or equal to ϕ_{sphere}. Thus, the anisotropy decay data indicate that a structural domain of VIIa that contains the active site undergoes segmental motions. Moreover, the anisotropy decay data indicate that these motions are damped when VIIa binds sTF. We suggest that this stabilization by the cofactor, TF, of a limited number of conformations of the enzyme VIIa is important for proper recognition of the substrate factor X.

ACKNOWLEDGMENTS

We appreciate the technical assistance of Theresa M. Ridgeway, Daryl Lyons, and Steven Eaton, and we wish to acknowledge the scientific contributions of Dr. Arabinda Guha, Dr. Carol Hasselbacher, and Dr. Donald Senear. We also thank one of the reviewers for their careful attention and helpful suggestions.

REFERENCES

Bach, R. (1988) *CRC Crit. Rev. Biochem. 23*, 339-368.

Badea, M. G., & Brand, L. (1979) *Methods Enzymol. 61*, 378-425.

Belford, G. G., Belford, R. L., & Weber, G. (1972) *Proc. Natl. Acad. Sci. U.S.A. 69*, 1392-1393.

Bevington, P. R. (1969) *Data Reduction and Error Analysis for the Physical Sciences*, pp. 204-246, McGraw-Hill, New York, NY.

Cohn, E. J., & Edsall, J. T. (1943) Proteins, Amino Acids and Peptides as Ions and Dipolar Ions, p. 157, Rheinhold, New York, NY.

Cross, A. J., & Fleming, G. R. (1984) *Biophys. J.* 46, 45-56.

Gemmell, C. H., Broze, G. J., Jr., Turitto, V.T., & Nemerson, Y. (1990) *Blood 76*, 2266-2271.

Hasselbacher, C. A., Waxman, E., Galati, L., Contino, P., Ross, J. B. A., & Laws, W. R., (1991a) *J.Phys. Chem. 95*, 2995-3005.

Hasselbacher, C. A., Schwatz, G. P., Glass, J. D., & Laws, W. R., (1991b) *Int. J. Peptide Protein Res. 38*, 459-468.

Husten, J. E., Esmon, C. T., & Johnson, A. E. (1987) *J. Biol. Chem. 27*, 12953-12961.

Isaacs, B. S., Husten, E. J., Esmon, C. T., & Johnson, A. E. (1986) *Biochemistry 25*, 4958-4969.

Johnson, M. L., Correia, J. C., Yphantis, D. A., & Halvorson, H. R. (1981) *Biophys. J. 36*, 575-588.

Lakowicz, J. R. (1983) *Principles of Fluorescence Spectroscopy*, pp. 161-162, Plenum Press, New York, NY.

Laue, T. M. (1981) , Ph.D. dissertation, University of Connecticut, Storrs, CT.

Laue, T. M., Johnson, A. E., Esmon, C. T., & Yphantis, D. A. (1984) *Biochemistry 23*, 1339-1348.

Laue, T. M., Shah, B. D., Ridgeway, T. M., and Pelletier, S. M. (1992) *Analytical Ultracentrifugation in Biochemistry and Polymer Science,* Eds. S. Harding & A. Rowe, Royal Society of Chemistry, London, *in press.*

Lim, T. K., Bloomfield, V. A., and Nelsestuen, G. L. (1977) *Biochemistry 25,* 4177-4181.

Luckow, E. A., Lyons, D. A., Ridgeway, T. M., Esmon, C. T. & Laue, T. M. (1989) *Biochemisty 28,* 2348-2354.

Nemerson, Y., & Turitto, V. T. (1991) *Thrombosis and Haemostasis 66,* 272-276.

Olsen, P. H., Esmon, N. L., Esmon,T., Laue, T. M. (1992) *Biochemistry 31,* 746-754.

Perrin, F. (1934) *J. Phys. Rad., Ser. VII,* **V**, 497-511.

Pessen, H., & Kumosinski, T. F. (1985) *Methods Enzymol. 117,* 219-255.

Silverberg, S. A., Nemerson, Y., & Zur, M. (1977) *J. Biol. Chem. 252,* 8481-8488.

Small, E. W., & Isenberg, I. (1977) *Biopolymers 16,* 1907-1928.

Stafford, W. F. III, & Szent-Györgyi, A.G. (1978) *Biochemistry 17,* 607-614.

Stafford, W. F. III (1992) *Anal. Biochem. 203,* 295-301.

Tao, T. (1969) *Biopolymers 8,* 609-632.

Teller, D. C. (1973) *Methods Enzymol.* 27, 346-441.

Teller, D. C. (1976) *Nature 260,* 729-731.

Thim, L., Bjoern, S., Christensen, M., Nicolaisen, E. M., Lund-Hansen, T., Pedersen, A. H., & Hedner, U. (1988) *Biochemistry 27,* 7785-7793.

Van Holde, K. E. (1985) *Physical Biochemistry,* 2nd. Ed. p. 117, Prentice-Hall, Englewood Cliffs, NJ.

Waxman, E., Ross, J. B. A., Laue, T. M., Guha, A., Thiruvikraman, S. V., Lin, T. C., Konigsberg, W. H., & Nemerson, Y. (1992) *Biochemistry 31,* 3998-4003.

Waxman, E., Laws, W.R., Laue, T.M., Nemerson, Y., & Ross, J.B.A. (1993) *Biochemistry 32,* 3005-3012.

Wetlaufer, D. B. (1962) *Adv. Prot. Chem. 17,* 303-390.

Yguerabide, J., Epstein, H.F., & Stryer, L. (1970) *J. Mol. Bio. 51*, 573-590.

Yphantis, D. A. (1960) *Ann. N.Y. Acad Sci. 88*, 586-601.

Yphantis, D. A. (1964) *Biochemistry 3*, 297-317.

CHAPTER 5

SUMMARY AND FURTHER DISCUSSION

Soluble tissue factor as a model for TF:VIIa interactions.

Chapter 3 of this work introduces sTF, a soluble TF mutant containing the extracellular domain of native TF, as a potential model for studying TF:VII(a) interactions in the absence of lipid. Under the conditions examined sTF was shown to have approximately 4% of the activity of TF. The possibility that the decreased activity might be accounted for by decreased affinity of VII(a) for sTF as compared to lipid-reconstituted full-length TF was investigated. The dissociation constant at 25° C for the sTF:VIIa complex was found to be 0.59 nM corresponding to a free energy for complex formation of -12.5 kcal mol^{-1}. The dissociation constant for the TF:VIIa was found to be 7.3 pM corresponding to a free energy of complex formation of -15.3 kcal mol^{-1}. The affinity of VII(a) for sTF is clearly decreased compared to that for lipid-reconstituted full-length TF. However, under the conditions with which the activity measurements were performed, the decreased affinity was not sufficient to account for the decreased activity of the sTF:VII(a) complex relative to TF:VII(a).

The 2.8 kcal mol^{-1} difference in the free energy of complex formation suggests the presence of additional interactions in the lipid-reconstituted full-length TF:VII(a) complex that are not present in sTF:VII(a). In addition, the pressure dissociation experiments in Chapter 3 show that the molar volume change for sTF:VIIa complex formation is -63 mL mol^{-1}, -54 mL mol^{-1} less than the -117 mL mol^{-1} seen for TF:VII(a) formation. As discussed in Chapter 2, certain affinity-increasing interactions between proteins result in larger molar volume changes on complex formation. The decreased molar volume change for sTF:VII(a) relative to TF:VII(a) is thus consistent with the hypothesis that sTF:VII(a)

has decreased electrostatic-type bonding and/or decreased surface to surface apposition.

An observation that points to the possible nature of the missing interaction is that sTF:VII(a) activity, but not complex formation, has an absolute dependence on the presence of lipid. The decrease in sTF:VII(a) activity relative to lipid-reconstituted full-length TF:VII(a), as well as the difference in thermodynamic parameters between the complexes, is likely to be due to differences in the way that sTF and sTF:VII(a) interacts with lipid.

What then, is the role for sTF as a model for further studies of TF and its interactions with VII(a)? Clearly, if the object of the creation of a soluble truncation mutant of TF had been to create a more experimentally convenient molecule identical to TF in all other respects, then sTF would be a grossly flawed model. The observations discussed above make it apparent that sTF:VII(a) complex is in some way structurally different than TF:VII(a). The nature of the structural differences, however, make it likely that sTF is an appropriate model for answering the sorts of questions it was originally designed to i.e., which aspects of TF:VII(a) activity are protein-protein mediated, which aspects are protein-lipid mediated and how the protein-protein and protein-lipid interaction impact upon each other.

Reciprocal regulation of the active site and the cofactor binding site of VIIa.

As discussed in Chapter 1, detailed kinetic studies of the activation of X by VIIa (Nemerson and Gentry, 1986) indicate that this reaction proceeds by a fully ordered mechanism in which VIIa undergoes two conformational changes. The first is associated

with the binding of VIIa to TF and results in the formation of a holoenzyme that can bind and turnover X. The second is associated with the binding of X to the TF:VIIa complex and results in the incerased affinity of VIIa for TF. This ordered addition, essential activation model was dubbed the "conformational cage" denoting that the dissociation of TF:VIIa is prevented when the active site of VIIa is occupied.

Chapter 4 of this work provides evidence for the first of these two conformational changes. In the absence of TF, a biexponential decay was observed for the time resolved fluorescence anisotropy of a dansyl probe attached at the active site of VIIa. At 20° C, the two time constants for the decay were 96 ns and 12 ns. Theory predicts that the anisotropy decay for a hydrated rigid spherical protein with the same molecular weight as VIIa would be monoexponential with a time constant of 23 ns. The 96 ns was thus attributed to the depolarizing effects of the rotation of VIIa as a whole and the 12 ns decay was attributed to the depolarizing effects due to the segmental motion of a domain containing the fluorescently labelled active site. The amount by which the time constant for the overall rotation exceeds that predicted for a sphere is an indicator of the high asymmetry of this protein. In the presence of saturating amounts of sTF the anisotropy decay was observed to be monoexponential with a time constant of 122 ns. The increase in this time constant relative to the time constant for overall rotation of VIIa alone is due to the larger volume of the complex. The loss of the shorter decay reflects the loss of the segmental motion in VIIa when it binds sTF. This is direct physical evidence that the binding of sTF to VIIa induces a conformational change in VIIa which restricts the segmental motions of a domain containing the active site.

The use of fluorescently labelled VIIa for the studies presented in this work raises the question of how the labelling might effect the physical properties of VIIa. Preliminary experiments addressing the question have provided intriguing results. Titration experiments at atmospheric pressure were performed by the addition of sTF or full-length PC-reconstituted TF to samples containing 40 nM DF-VIIa in the absence and presence of 40 or 150 nM competing unlabelled VIIa. Simultaneous analysis of the data from the experiments performed in the presence of unlabelled VIIa indicate that the dissociation constant for the complex formed by sTF and unlabelled VIIa complex is in the range of 4 to 8 nM. Experiments using lipid-reconstituted full-length TF suggest a similar increase in the dissociation constant for the complex with unlabelled relative to labelled VIIa. This provides direct physical evidence that occupation of the active site of VIIa induces a conformational change in VIIa the increases its affinity for TF.

As discussed in chapter 3, the mechanism of action of TF is described by some authors as that of a "receptor" for VIIa. In the receptor model of TF action, docking of VIIa to transmembrane TF without concomitant conformational change in VIIa is sufficient to endow it with enhanced proteolytic activity. The interaction between VIIa and TF is thus passive, in that model, and the enhanced activity derives solely from facilitation of assembly of the cofactor:enzyme:substrate complex, TF:VII:X, on the membrane surface. The earlier kinetic data by Nemerson and Gentry and the physical data presented here are in direct conflict with this model. These data provide evidence for reciprocal regulation of the active site and the TF-binding site of VIIa. That is, occupation of the active site of VIIa alters the affinity of its TF-binding site, while

occupation of the binding site for TF alters the active site affinity for substrate of VIIa. Clearly, a model in which TF is a passive docking site is ruled out by these data.

Directions for future experiments.

It is my hope that the experiments discussed in this work will provide stimulus for further work in this area. The techniques and reagents developed for the studies presented in chapter 3 make possible a wide variety of experiments addressing the mechanism and regulation of TF:VIIa binding. Extension of the thermodynamic studies presented in Chapter 3 to include the temperature dependence of the free energy and molar volume changes of complex formation would lead to further insight into the nature of the protein-protein interactions responsible for active TF:VIIa complex formation. Similar experiments performed with either full-length TF or sTF in the presence of micelles of different compositions will help to clarify the role of negatively charged lipids in TF:VIIa and sTF:VIIa activity.

Application of the techniques developed in Chapter 4 to investigate a fluorescently labelled sTF will make it possible to observe the hydrodynamics of sTF:VIIa complex from the perspective of the cofactor. As yet, there is no evidence as to the shape or structure of TF. Neither is there any evidence of a concomitant structural change in TF upon binding VIIa.

Perhaps most exciting are the possibilities suggested by the preliminary competition studies presented above in this chapter. The mechanism of the conformational cage could be explored in depth by comparison of TF:VIIa complex formation in the

presence of a series of inhibitors of VIIa. Competition studies in which DF-VIIa affinity of TF or sTF is compared to the affinity of VIIa in the presence of inhibitors ranging from benzamidine to an uncleavable X or large excess of Xa could be used to probe the specificity of the conformational cage mechanism.

References

Azumi, T. & McGlynn, S. P. (1962) *J. Chem. Phys. 37*, 2413-2420.

Bach, R., Nemerson, Y., & Konigsberg, W. (1981) *J. Biol. Chem. 256*, 8324-8331.

Bach, R., Oberdick, J. and Nemerson, Y. (1984) *Blood*, 63, 393-398.

Bach, R., Gentry, R., & Nemerson, Y. (1986) *Biochemistry 25*, 4007-4020.

Bach, R. (1988) Initiation of coagulation by Tissue Factor *CRC Crit. Rev. Biochem. 23*, 339-368.

Bach, R., Konigsberg, W. H., & Nemerson, Y. (1988) *Biochemistry 27*, 4227-4231.

Bach, R. (1988) *CRC Crit. Rev. Biochem.* 23, 339-368.

Badea, M. G., & Brand, L. (1979) *Methods Enzymol. 61*, 378-425.

Belford, G. G., Belford, R. L., & Weber, G. (1972) *Proc. Natl. Acad. Sci. U.S.A. 69*, 1392-1393.

Benson, A.M., and Drickamer, H.G. (1957) *J Chem. Phys. 27*, 1164-1174

Berkner, K., Busby, S., Davie, E., Hart, C., Insley, M., Kisiel, W., Kumar, A., Murray, M., O'Hara, P., Woodbury, R. (1986) *Cold Spring Harbor Symposia on Quantitative Biology* 51, 531-541.

Bevington, P. R. (1969) *Data Reduction and Error Analysis for the Physical Sciences*, pp. 204-246, McGraw-Hill, New York, NY.

Bevington, P. R. (1969) *Data Reduction and Error Analysis for the Physical Sciences*, pp. 204-246, McGraw-Hill, New York, NY.

Broze, G.J., and Majerus, M.J. (1980) *J. Biol. Chem.* 255, 1242-1247.

Broze, G. J., (1982) *J. Clin. Invest. 70*, 526-535.

Broze, G.J., Jr., Leykam, J.E., Schwartz, B.D., & Miletich, J.P. (1985) *J. Biol. Chem.* 260, 10917-10920.

Cohn, E. J., & Edsall, J. T. (1943) Proteins, Amino Acids and Peptides as Ions and Dipolar Ions, p. 157, Rheinhold, New York, NY.

Cross, A. J., & Fleming, G. R. (1984) *Biophys. J.* 46, 45-56.

Davie, E.W. (1986) *J. Protein Chem.* 5, 247-253

Deranleau, D. (1969) *J. Am. Chem. Soc.* 91 4044-4049.

Di Scipio, R. G., Hermodson, M. A., Yates, S. G., & Davie, E. W. (1977) *Biochemistry 16,* 698-705.

Edgington, T. S., Mackman, N., Brand, K., & Ruf, W. (1991) *Thromb. and Haem. 66,* 67-79.

Fair, D. S., & MacDonald, M. J. (1987) *J. Biol. Chem. 262,* 11692-11698.

Fisher, K.L., and Gorman, C.M. (1989) *Thromb. Res.* 48, 89-99.

Gemmell, C. H., Broze, G. J., Jr., Turitto, V.T., & Nemerson, Y. (1990) *Blood 76,* 2266-2271.

Guha, A., Bach, R., Konigsberg, W., & Nemerson, Y., (1986) *Proc. Natl. Acad. Sci. U.S.A.* 83, 299-302.

Hagen, F.S., Gray, C.L., O'Hara, P., Grant, F.J., Saari, G.C., Woodbury, R.G., Hart, C.E., Insley, M., Kisiel, W. (1986) *Proc. Natl. Acad, Sci. U.S.A.* 83, 2412-2416.

Hasselbacher, C. A., Waxman, E., Galati, L., Contino, P., Ross, J. B. A., & Laws, W. R., (1991a) *J.Phys. Chem. 95,* 2995-3005.

Hasselbacher, C. A., Schwatz, G. P., Glass, J. D., & Laws, W. R., (1991b) *Int. J. Peptide Protein Res. 38,* 459-468.

Heremans, K. (1982) *Ann. Rev. Biophys. Bioeng. 11,* 1-21.

Husten, J. E., Esmon, C. T., & Johnson, A. E. (1987) *J. Biol. Chem. 27,* 12953-12961.

Isaacs, B. S., Husten, E. J., Esmon, C. T., & Johnson, A. E. (1986) *Biochemistry 25,* 4958-4969.

Jackson, C. and Nemerson, Y. (1980) *Ann Rev. Biochem.* 49, 765-811.

Johnson, M. L., Correia, J. C., Yphantis, D. A., & Halvorson, H. R. (1981) *Biophys. J. 36,* 575-588.

Lakowicz, J. R. (1983) *Principles of Fluorescence Spectroscopy*, pp. 161-162, Plenum Press, New York, NY.

Laue, T. M. (1981) , Ph.D. dissertation, University of Connecticut, Storrs, CT.

Laue, T. M. (1981) *"Rapid Precision Interferometry for the Analytical Ultracentrifuge"*, Ph.D. dissertation, University of Connecticut, Storrs, CT.

Laue, T. M., Johnson, A. E., Esmon, C. T., & Yphantis, D. A. (1984) *Biochemistry 23,* 1339-1348.

Laue, T. M., Shah, B. D., Ridgeway, T. M., and Pelletier, S. M. (1992) *Analytical Ultracentrifugation in Biochemistry and Polymer Science,* Eds. S. Harding & A. Rowe, Royal Society of Chemistry, London, *in press.*

Lim, T. K., Bloomfield, V. A., and Nelsestuen, G. L. (1977) *Biochemistry 25*, 4177-4181.

Lerner, R.G., Goldstein, R., and Cummings, G. (1971) *Proc. Soc. Exp. Biol. Med.* 138, 145-148.

Luckow, E. A., Lyons, D. A., Ridgeway, T. M., Esmon, C. T. & Laue, T. M. (1989) *Biochemisty 28*, 2348-2354.

Mann, K. G. , Nesheim, M. E., Church, W. R., Haley, P., & Krishnaswamy, S. (1990) *Blood 76*, 1-16.

Messing, J., (1983) *Methods Enzymol. 101,* 20-78.

Miletich, J. P., Broze, G. J., & Majerus, P. W. (1981) *Methods Enzymol. 80*, 221-228.

Mimms, L. T., Zampighi, G., Nozaki, Y., Tanford, C., & Reynolds, J. A. (1981) *Biochemistry 20*, 833-840.

Morild, E. (1981) *Advances in Protein Chemistry* 34, 93-166.

Morrisey, J.H., Fakhrai, H. and Edgington T.S. (1987) *Cell,* 50, 129-135.

Morrissey, J. H., Fair, D. S., & Edgington, T. S. (1988) *Thrombosis Research 52,* 247-261.

Nemerson, Y. & Gentry, R. (1986) *Biochemistry* 25, 4020-4033.

Nemerson, Y. (1988) *J. Am. Soc. Hematology* 71, 1-8.

Nemerson, Y., & Turitto, V. T. (1991) *Thrombosis and Haemostasis 66*, 272-276.

Olsen, P. H., Esmon, N. L., Esmon,T., Laue, T. M. (1992) *Biochemistry 31*, 746-754.

Paladini, A. A., & Weber, G. (1981) *Rev. Sci. Inst. 52*, 419-427.

Paladini, A. and Weber, G. (1983) *Methods in Enzymology* 53, 419-427.

Paoletti, J., & LePecq, J. B. (1969) *Anal. Biochem. 31*, 33-41.

Perrin, F. (1934) *J. Phys. Rad., Ser. VII*, V, 497-511.

Pessen, H., & Kumosinski, T. F. (1985) *Methods Enzymol. 117*, 219-255.

Ploplis, V. A., Edgington, T. S., & Fair, D. S. (1987) *J. Biol. Chem. 262*, 9503-9508.

Rodgers., G. M., Broze, G. J., & Shuman, M. A. (1984) *Blood 63*, 434-438.

Rosing, J., Tans, G., Govers-Riemslag, W. P., Zwaal, R. F. A., & Hemker, H. C. (1979) *J. Biol. Chem. 255*, 274-283.

Ruf, W., Kalnik, M. W., Lund-Hansen, T., & Edgington, T. S. (1991) *J. Biol. Chem. 266*, 15719-15725.

Ruf, W., Rehemtulla, A., & Edgington, T. S. (1991a) *J. Biol. Chem. 266*, 2158-2166.

Ruf, W., Kalnik, M. W., Lund-Hansen, T., & Edgington, T. S. (1991b) *J. Biol. Chem. 266*, 15719-15725.

Scarpati, E.M., Wen D., Broze, G.J., Mileteich, J.P., Flandermeyer, R.R., Siegel, N.R., and Sadler, J.E. (1987) *Biochemistry*, 26, 5234-5238.

Spicer, E. K., Horton, R., Bloem, L., Bach, R., Williams, K. R., Guha, A., Kraus, J., Lin, T. C., Nemerson, Y., & Konigsberg, W. H. (1987) *Proc. Natl. Acad. Sci. U.S.A. 84*, 5148-5152.

Silverberg, S. A., Nemerson, Y., & Zur, M. (1977) *J. Biol. Chem. 252*, 8481-8488.

Small, E. W., & Isenberg, I. (1977) *Biopolymers 16*, 1907-1928.

Spicer, E. K., Horton, R., Bloem, L., Bach, R., Williams, K. R., Guha, A., Kraus, J., Lin, T. C., Nemerson, Y., & Konigsberg, W. H. (1987) *Proc. Natl. Acad. Sci.*

U.S.A. 84, 5148-5152.

Stafford, W. F. III, & Szent-Györgyi, A.G. (1978) *Biochemistry 17,* 607-614.

Stafford, W. F. III (1992) *Anal. Biochem. 203,* 295-301.

Tao, T. (1969) *Biopolymers 8,* 609-632.

Teller, D. C. (1973) *Methods Enzymol.* 27, 346-441.

Teller, D. C. (1976) *Nature 260,* 729-731.

Thim, L., Bjoern, S., Christensen, M., Nicolaisen, E. M., Lund-Hansen, T., Pedersen, A. H., & Hedner, U. (1988) *Biochemistry 27,* 7785-7793.

Van Holde, K. E. (1985) *Physical Biochemistry,* 2nd. Ed. p. 117, Prentice-Hall, Englewood Cliffs, NJ.

Warn-Cramer, B. J., & Bajaj, S. P. (1986) *Biochem. J. 239,* 757-762.

Waxman, E., Ross, J. B. A., Laue, T. M., Guha, A., Thiruvikraman, S. V., Lin, T. C., Konigsberg, W. H., & Nemerson, Y. (1992) *Biochemistry 31,* 3998-4003.

Waxman, E., Laws, W.R., Laue, T.M., Nemerson, Y., & Ross, J.B.A. (1993) *Biochemistry 32,* 3005-3012.

Weber, G., and Drickamer, H.G., (1983) *Quart. Rev. Biophys.* 16, 89-112.

Wetlaufer, D. B. (1962) *Adv. Prot. Chem. 17,* 303-390.

Yanis-Perron, C., Biera, J., & Messing, J. (1985) *Gene 33,* 103-119.

Yguerabide, J., Epstein, H.F., & Stryer, L. (1970) *J. Mol. Bio. 51,* 573-590.

Yphantis, D. A. (1960) *Ann. N.Y. Acad Sci. 88,* 586-601.

Yphantis, D. A. (1964) *Biochemistry 3,* 297-317.

Zur, M. and Nemerson, Y. (1981) *Haemostasis and Thrombosis,* A. L. Bloom and D. P. Thomas (Eds.), pp 124-142, Churchill Livingston, Edinburgh.